MAUSAM, **77**, 3 (July 2026), 939-960

MAUSAM

DOI: https://doi.org/10.54302/mausam.v77i3.6977
Homepage: https://mausamjournal.imd.gov.in/index.php/MAUSAM

UDC No.551.577.38:551.583(540.29)

# Assessing drought trends and prediction using GCMs: A case study of South Bihar

HARI PRAKASH[1], PRAMOD SONI[2] and K. K. PANDEY[3]

[1]*Research Scholar, Department of Civil Engineering IIT BHU, Varanasi (U.P),221005,India,*

[2]*Assistant Professor,Department of Civil Engineering IIT BHU, Varanasi(U.P),221005, India*

[3]*Associate Professor, Department of Civil Engineering, IIT BHU, Varanasi (U.P),221005,India*

(*Received 25 February 2025, Accepted 1 December 2025*)

***Corresponding author's email: hariprakash.rs.civ23@iitbhu.ac.in**

**सार** – दक्षिण बिहार जैसे अर्ध-शुष्क क्षेत्रों में जलवायु परिवर्तन के तहत वर्षण के अनुमानों को समझना जल-संसाधन योजना के लिए अत्यंत महत्वपूर्ण है। यह अध्ययन 14 डाउनस्केल्ड, क्षेत्रीय रूप से समायोजित वैश्विक जलवायु मॉडलों (GCMs) के आउटपुट का उपयोग करके दक्षिण बिहार के दक्षिणी जिलों में सूखे के प्रतिरूपों पर एक उच्च-उत्सर्जन परिदृश्य (RCP 8.5) के प्रभावों की जांच करता है। मौसम संबंधी सूखे को मानकीकृत वर्षण सूचकांक (Standardized Precipitation Index - SPI) द्वारा अभिलक्षित किया गया है। वर्ष 2006-2020 के लिए भारत मौसम विज्ञान विभाग (IMD) के अवलोकनों के साथ GCM वर्षण को सहसंबद्ध करके मॉडल के प्रदर्शन का मूल्यांकन किया गया था; सर्वश्रेष्ठ प्रदर्शन करने वाले मॉडल HadGEM2-AO, MRI-CGCM3, MIROC5, CESM1-CAM5 और CCSM4 थे। अनुमान संकेत देते हैं कि हल्के से मध्यम सूखे की गंभीरता में लगभग ~30% की वृद्धि होगी, जिसमें गया, जमुई और लखीसराय सबसे अधिक प्रभावित होंगे। वर्ष 2021-2050 के दौरान वर्षा रहित अवधियों की संभावना बढ़ने का अनुमान है, जो शुष्क अवधि से प्रेरित मौसम संबंधी सूखे के बढ़ते जोखिम का संकेत देता है। हालांकि प्रत्येक सूखे की घटनाओं की नियतात्मक (Deterministic) भविष्यवाणी नहीं की जा सकती है, लेकिन बदलती वर्षा प्रणाली आर्द्र और शुष्क स्थितियों के बीच अधिक उतार-चढ़ाव का सुझाव देती है। अनुकरण (सिमुलेटेड) तथा प्रेक्षित (ऑब्ज़र्व्ड) वर्षा के बीच उच्च स्तर की समानता ($R^2 \approx 0.63$-$0.73$) इस क्षेत्र में भविष्य के सूखा जोखिम के आकलन के लिए इन मॉडलों की उपयुक्तता का समर्थन करती है।

**ABSTRACT.** Understanding precipitation projections under climate change in semi-arid regions such as South Bihar is crucial for water-resources planning. This study examines the impacts of a high-emissions scenario (RCP 8.5) on drought patterns across the southern districts of Bihar using outputs from 14 downscaled, regionally adjusted global climate models (GCMs). Meteorological drought is characterized with the Standardized Precipitation Index (SPI). Model performance was evaluated by correlating GCM precipitation with India Meteorological Department (IMD) observations for 2006–2020; the best-performing models were HadGEM2-AO, MRI-CGCM3, MIROC5, CESM1-CAM5, and CCSM4. Projections indicate an ~30% increase in the severity of mild-to-moderate droughts, with Gaya, Jamui, and Lakhisarai most affected. The likelihood of rainless spells during 2021–2050 is projected to rise, signalling a growing risk of dry spell driven meteorological drought. While individual drought events cannot be predicted deterministically, the evolving rainfall regime suggests greater alternation between wet and dry conditions. Strong agreement between simulated and observed precipitation ($R^2 \approx 0.63$–$0.73$) supports the suitability of these models for assessing future drought risk in this region.

**Key words** - Climate change, Meteorological Drought, SPI, GCMs, South Bihar.

## 1. Introduction

Climate change is a critical driver of variability in plant development, growth, and ultimately crop yield and quality, especially under drought stress (Fahad *et al*. 2022)**.** By disrupting soil–plant–atmosphere interactions, it is impairing agricultural operations, reducing production, and contributing to higher food prices

worldwide (Clair *et al*. 2010; Newton *et al*., 2011). Sustained gains in agricultural productivity and rural livelihoods therefore require sustainable soil and water management Kar *et al.* (2022)**.** Drought is a phenomenon characterized by prolonged periods of hydro-meteorological parameter imbalances resulting from continuous episodes of dry seasons and limited rainfall Mishra and Singh (2010). It is commonly classified into four types of drought which can be classified as meteorological, agricultural, hydrological, and socio-economic droughts (Wilhite and Glantz 1985; Mishra and Desai 2005). Meteorological drought refers to extended periods of below-normal precipitation and is characterized by the magnitude of departure from normal and the duration of dry spells; it elevates wildfire risk, depletes soil moisture, and stresses vegetation (Santos 1983; Chang 1991). Meteorological drought is often described by the degree of dryness (in comparison to some "normal" or average amount) and the length of the dry period that can raise the risk of wildfires, reduce soil moisture, and have an influence on vegetation health. Hydrological drought manifests as reduced streamflow, reservoir storage, and groundwater levels and often follows extended rainfall shortages (Alamgir *et al*., 2020; Hayes *et al*., 1999). These moisture deficits propagate through the water cycle, driving agricultural drought via soil-moisture depletion, crop failure, and reduced water availability Van Dijk *et al*. (2013).

Regionalization-classifying space into zones with similar drought behavior, helps identify adjacent areas with comparable characteristics and supports targeted risk management (Aon and Biswas, 2023). Meteorological drought exhibits complex spatial organization, with diverse areal extents and spatial patterns (Vicente-Serrano 2006). Globally, numerous studies have analyzed the spatio-temporal variability of drought using regional classification techniques such as principal component analysis and mesoscale pattern typing (Cheval *et al*., 2014; Debanli *et al.* (2017); Kalisa *et al*., 2020; Merabti *et al*., 2018; Mustafa and Rahman 2018). In India, several works have applied the Standardized Precipitation Index (SPI) to assess spatio-temporal drought dynamics (Mishra and Desai, 2005; Mishra and Nagarajan, 2011; Thomas *et al*., 2015; Mahajan and Dodamani 2016; Gupta and Jain, 2018:2019; Anandharuban and Elango 2021). However, comprehensive regionalization coupled with detailed regional drought-frequency analysis prior to characterization remains limited. Additional SPI-based regional assessments include Rajasthan (Mundetia and Sharma, 2015) and the impacts of drought on rice productivity in Odisha (Raja *et al*., 2014).

Global Climate Models (GCMs) are powerful numerical tools that employ three-dimensional representations of physical processes within the land surface, ocean, and atmosphere. GCMs have been developed to simulate the current climate and its effects on climatic variables within hydrological networks, enabling researchers to address climate change and its impacts (Charles *et al*., 2010; Hayes *et al*., 1999). The latest phase of the Coupled Model Intercomparison Project, CMIP6, offers improved simulations of historical variability and future projections (Raju and Kumar, 2014; Patel *et al*., 2023; Salehie *et al*., 2023). Compared with CMIP5, CMIP6 features a new generation of models, a later historical end/start year ( 2015 for CMIP6 vs. 2006 for CMIP5), and an updated scenario framework for concentrations, emissions, and land use Gidden *et al*. (2019). However, uncertainties remain regarding how well CMIP6 models capture the climate response to anthropogenic forcing over South Asia (Allabakash and Lim, 2022). In India, numerous studies have combined SPI with GCM outputs to examine meteorological drought. For example (Laddimath and Patil, 2020) assessed future meteorological drought in the Bhima basin using CMIP6 multi-model projections, and (Saharwardi and Kumar, 2022), evaluated future drought changes and associated uncertainties across India's homogeneous regions. These studies generally compute drought severity with SPI and project increases in drought intensity and frequency under high-emissions scenarios.

However, prior studies have not quantified drought magnitude at individual stations for both historical observations and future projections. Focusing on South Bihar, we address this gap and find growing vulnerability to drought, warranting a thorough assessment of severity. Accordingly, this study conducts a station-by-station, spatio-temporal evaluation of drought severity using the Standardized Precipitation Index (SPI) at 1-, 3-, 6-, and 12-month time scales.

In this study, we developed a GCM-ranking framework that integrates three multi-criteria decision-making (MCDM) methods Compromise programming (CP), Cooperative game theory (CGT), and the Technique for order preference by similarity to ideal solution (TOPSIS) to evaluate model skill using simulated precipitation. Unlike prior work, this combined scheme provides a more comprehensive and nuanced assessment across multiple performance indicators. We focus on CMIP5 owing to its longer and more recent historical coverage, updated scenario framework, and practical data availability for the region (Balaji *et al*., 2018), while noting the scarcity of station-scale precipitation modeling tailored to Bihar. Therefore, this study aims

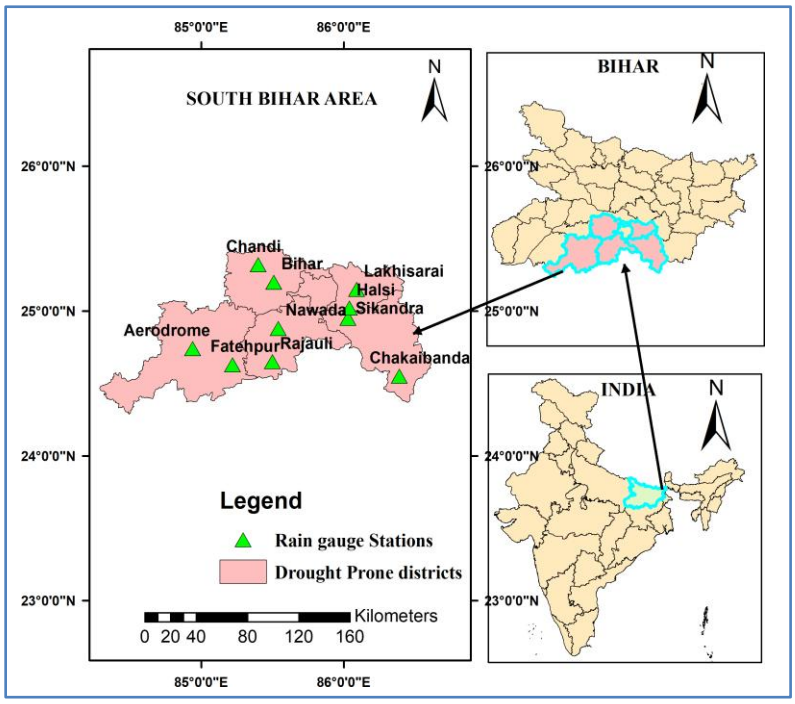


**Fig. 1.** Location map of the South Bihar study area

To analyze meteorological drought in five districts of South Bihar using the Standardized Precipitation Index (SPI).

To Identify and rank the most suitable CMIP5 GCMs at each station by combining multiple statistical performance indicators and assessing their influence on the rankings.

To project drought conditions for 2021–2050 under the RCP 8.5 scenario using the selected GCM ensemble.

## 2. Data and methodology

### 2.1. *Study area*

This study focuses on Bihar, a state in eastern India (area: 94,163 km²; mean elevation ~150 m). The climate is humid subtropical, with hot, dry summers and cool winters. Our analysis centers on South Bihar (14,385 km²; 84.0°–87.5° E, 24.0°–25.0° N), encompassing five districts-Gaya, Jamui, Lakhisarai, Nalanda, and Nawada (Fig.1;Table 1. Although both Bihar and South Bihar share a humid subtropical regime, notable gradients exist. State wise, seasonal variability is pronounced, and northern districts influenced by Himalayan foothill circulation and major rivers are more flood-prone. By contrast, South Bihar is relatively hotter and drier, with longer, more intense summers (often >40 °C), cooler winters (5-10 °C), and lower annual rainfall (≈800-1300 mm versus a state average of ~1120 mm). These conditions increase the region's drought susceptibility, motivating our focus on South Bihar. Most rainfall occurs during the southwest monsoon (June–September).

**TABLE 1**

**IMD Stations**

| S.no | Station | Latitude | Longitude | Elevation(m) |
|---|---|---|---|---|
| 1 | Aerodrome | 24.74°N | 84.94°E | 116 |
| 2 | Fatehpur | 24.63°N | 85.22°E | 150 |
| 3 | Chakaibanda | 24.55°N | 86.39°E | 82 |
| 4 | Sikandra | 24.95°N | 86.03°E | 56 |
| 5 | Halsi | 25.02°N | 86.04°E | 46 |
| 6 | Lakhisarai | 25.15°N | 86.09°E | 77 |
| 7 | Bihar | 25.20°N | 85.51°E | 55 |
| 8 | Chandi | 25.32°N | 85.40°E | 47 |
| 9 | Nawada | 24.88°N | 85.54°E | 80 |
| 10 | Rajauli | 24.65°N | 85.50°E | 135 |

### 2.2. *Data used*

We used monthly precipitation observations from the India Meteorological Department (IMD), Pune (Data Supply Portal: https://dsp.imdpune.gov.in) for 1975–2020 to analyze historical meteorological drought. Future

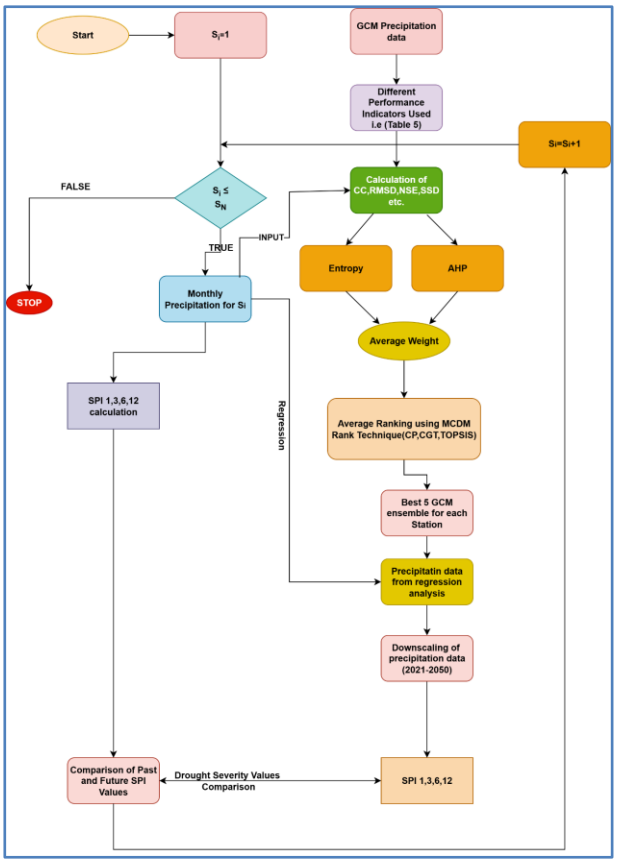


**Fig. 2.** SPI Drought calculation and detailed methodology

projections were obtained from 14 Coupled Model Intercomparison Project Phase 5 (CMIP5) global climate models via the ESGF node (https://aims2.llnl.gov/search), analyzed under the high-emissions RCP 8.5 scenario.

### 2.3. *Methodology*

This study employs the Standardized Precipitation Index (SPI), a widely used drought metric in meteorological and hydrological services worldwide. Because SPI standardizes precipitation anomalies, it enables consistent comparison of drought conditions across regions and time scales. Introduced by (McKee *et al*. 1993) and was authorized by the World Meteorological Organization (WMO) in 2011 for use in drought categorization. SPI is computed by fitting a two-parameter gamma distribution to aggregated monthly precipitation (for a chosen accumulation window), converting the cumulative probability to a standard normal variate (mean = 0, SD = 1). The gamma model has been shown to fit precipitation well (McKee *et al*. 1993; Stagge *et al*. 2015; Yacoub and Tayfur 2017). Months with zero precipitation are handled *via* a mixed-distribution adjustment before transformation. For robust estimation, (Guttman (1998) recommends that at least 40-60 years of precipitation data t stabilize the central portion of the distribution and roughly 70-80 years for the tails.

The non-parametric Mann–Kendall (MK) test is widely used to detect monotonic (increasing or decreasing) trends in time-series data without assuming a specific distribution. It compares the ranks of all observation pairs; a positive z-statistic indicates an upward trend and a negative value a downward trend. Statistical significance is assessed via the p-value, with $p < 0.05$ commonly used to reject the null hypothesis of no trend. Owing to its robustness to non-normality, outliers, and missing values, the MK test is well suited to hydroclimatic variables such as rainfall and temperature.

The flowchart which is shown in Fig. 2. depicts a comprehensive procedure for analyzing meteorological data, focusing primarily on Monsoonal precipitation patterns and drought indices, also making predictions for future climate scenarios. Initially, the process iterates over each of the 10 meteorological stations, acquiring monthly precipitation data from IMD Pune and calculating Standardized Precipitation Index (SPI) values for multiple time scales, especially for Monsoon seasons *i.e*. SPI 1(June month), SPI 3(June, July and August Months), SPI 6(June-November) and SPI 12(January-December). Future projections are made using GCM CMIP5 precipitation data which is easily available, followed by rigorous performance evaluation using various metrics like correlation coefficient, RMSD, and NSE given in TABLE 5. Indicators are calculated for each station, and average weights are determined using Entropy and Analytical Hierarchy Process (AHP). An ensemble approach was utilized further by using the values of the top 5 models for precipitation data and downscaled using polynomial regression. The SPI was recalculated for different time scales based on the downscaled data, and comparisons were done with historical data to analyze drought conditions.

The probability density function of the gamma distribution is shown below:

$$(x) = \frac{1}{\beta^{x}\,\Gamma(\alpha)} x^{\alpha-1} e^{-\frac{x}{\beta}} \quad \text{for x>0} \qquad (1)$$

where $\alpha > 0$ is the shape factor, $\beta > 0$ is a scale factor, $x > 0$ as the amount of precipitation.

$\Gamma(\alpha)$ is the gamma function which is defined as

$$\Gamma(\alpha) = \int_0^{\infty} y^{\alpha-1}\, e^{-y}.dy \qquad (2)$$

**TABLE 2**

**Global Climate Models (GCMs) used in this Study**

| No. | Institution | Model name | Resolution ($lat^0$ × $long^0$) |
|---|---|---|---|
| 1 | Institute Pierre-Simon Laplace, France | IPSL-CM5A-MR | 2.5×1.2676 |
| 2 | National Centre for Atmospheric Research, USA | CCSM4 | 1.25×.9424 |
| 3 | Institute for Numerical Mathematics, Russia | INM-CM4 | 2×1.50 |
| 4 | Beijing Climate Centre, China Meteorological Administration | BCC-CSM1-CAM5 | 2.8×2.8 |
| 5 | Community Earth System Model Contributors, NCAR USA | CESM1-CAM5 | 1.25×0.9424 |
| 6 | Commonwealth Scientific and Industrial Research Organization with Queensland Climate Change Centre of Excellence | CSIRO Mk3.6.0 | 1.875×1.875 |
| 7 | NASA Goddard Institute for Space Studies | GISS-E2-H | 2.5×2.0 |
| 8 | National Institute of Meteorological Research/Korea Meteorological Administration | HADGEM2-AO | 1.25×1.875 |
| 9 | Japan Agency for Marine-Earth Science and Technology | MIROC-ESM-CHEM | 2.8×2.8 |
| 10 | National Institute for Environmental Studies | MIROC-ESM | 2.8×2.8 |
| 11 | Atmospheric and Ocean Research Institute, The University of Tokyo | MIROC5 | 1.4×1.4 |
| 12 | Max Planck Institute for Meteorology, Germany | MPI-ESM-LR | 1.25×.9424 |
| 13 | Meteorological Research Institute, Japan | MRI-CGCM3 | 1.25×1.25 |
| 14 | Norwegian Meteorological Institute, Norway | NOrESM1-M | 2.5×1.875 |

To fit the distribution to the data, α and β values must be estimated. (Edwards 1997) proposed the following approach for estimating these parameters using (Thom 1958) approximation for maximum likelihood:

$$\hat{\alpha} = \frac{1}{4A}\left(1 + \sqrt{1 + \frac{4A}{3}}\right) \quad (3)$$

$$\hat{\beta} = \frac{\bar{x}}{\hat{\alpha}} \quad (4)$$

**(**where $S_i$= $i^{th}$ station $S_N$= Total Number of station)

**TABLE 3**

**Mann-Kendall Trend test for Meteorological Stations**

| Stations | z | n | p |
|---|---|---|---|
| RAJAULI | -2.67 | 46 | 0.007 |
| NAWADA | -1.53 | 46 | 0.125 |
| CHANDI | -2.21 | 46 | 0.026 |
| BIHAR | -0.07 | 46 | 0.939 |
| LAKHISARAI | 1.74 | 46 | 0.08 |
| HALSI | -1.13 | 46 | 0.255 |
| SIKANDRA | -3.07 | 46 | 0.002 |
| CHAKAIBANDA | -2.78 | 46 | 0.005 |
| FATEHPUR | -3.44 | 46 | 0.0005 |
| AERODROME | -2.53 | 46 | 0.025 |

**TABLE 4**

**Defining the severity of drought based on SPI value (Shah, Bharadiya, and Manekar 2015)**

| SPI VALUES | DROUGHT INDEX |
|---|---|
| >2 | Extreme Wet |
| 1.50 to 1.99 | Very Wet |
| 1.00 to 1.49 | Moderately Wet |
| -0.99 to 0 | Mild Dry |
| -1.49 to -1.00 | Moderately Dry |
| -1.99 to -1.50 | Severely Dry |
| < -2 | Extreme Dry |

where,

$$A = ln(\bar{x}) - \frac{\sum_{i=1}^{n} ln(x)}{n} \quad (5)$$

For $n$ observations, the following derivation is utilised. After that, the derived parameters are utilized to compute the cumulative probability of precipitation & event that has been observed. For a specific month or any other period: -

$$G(x) = \int_0^x g(x) \cdot dx = \frac{1}{\beta^x \Gamma\alpha} \int_0^x x^{\alpha-1} \cdot e^{-\frac{x}{\beta}} \cdot dx \quad (6)$$

Now, putting the value of t for $t = x / \hat{\beta}$ gives the value in equation (7) to an incomplete gamma function as given below, the cumulative distribution function is then given by:

$$G_{(x)} = \frac{1}{\Gamma(\hat{\alpha})} \int_0^x t^{\alpha-1} \cdot e^{-t} \cdot dt \quad (7)$$

Because the gamma function is essentially not defined for $x$ = 0, and a precipitation distribution may

**TABLE 5**

**Performance indicators used in the study**

| S.no | Statistical performance indicator | Formula | Notations |
|---|---|---|---|
| **1.** | Correlation coefficient (CC) | $\frac{\sum_{i=0}^{T}(x_i-\bar{x})(y_i-\bar{y})}{(\mathbf{T}-\mathbf{1})\cdot s_0\cdot s_s}$ | So, and Ss, standard deviations of historic and simulated values. T is the no. of dataset x= number of datasets. |
| **2.** | Nash Sutcliffe Model Efficiency (NSE) | $1-\frac{\sum_{i=1}^{T}(x_i-y_i)^2}{\sum_{i=1}^{T}(x_i-\bar{x})^2}$ | i, dataset number varying from 1,2 . …. x<br>$\bar{x}$, and y, are mean values of historical and simulated |
| **3.** | Sum of Squares of Deviation (SSD) | $\sum_{i=1}^{T}(x_i-y_i)^2$ | $x_i$ and $y_i$ are observed and simulated values respectively. T is number of datasets. |
| **4.** | Mean Square Deviation (MSD) | $\frac{1}{T}\sum_{i=1}^{T}(x_i-y_i)^2$ | $x_i$ and $y_i$ are observed and simulated values respectively. T is number of datasets. |
| **5.** | Normalised Root Mean Square Deviation(NRMSD) | $\frac{\sqrt{\left(\frac{1}{T}\right)\sum_{i=1}^{T}(x_i-y_i)^2}}{\bar{x}}$ | $\bar{x}$ and y, are mean values of historic and simulated; |
| **6.** | Absolute Normalised Mean Biased Deviation (ANMBD) | $\left\lvert\frac{\frac{1}{T}\sum_{i=1}^{T}(y_i-x_i)}{\bar{x}}\right\rvert$ | $x_i$ and $y_i$, are historic and simulated value. |
| **7.** | Root Mean Square Deviation (RMSD) | $\sqrt{\frac{1}{T}\sum_{i=1}^{T}(x_i-y_i)^2}$ | $x_i$ and $y_i$ are observed and simulated values respectively. T is number of datasets. |
| **8.** | Average Absolute Relative Déviations (AARD) | $\frac{1}{T}\sum_{i=i}^{T}\left\lvert\frac{(y_i-x_i)}{x_i}\right\rvert$ | $x_i$ and $y_i$ are observed and simulated values respectively. T is number of datasets. |

*$k_j(a)$ =Value of indicator j for GCM a; $r_j$ =Weight assigned to the indicators. $K_j^{**}$ = Anti ideal value for each indicator and j=1, 2…J where J is the number of indicators*

contain zeros Shah *et al*. (2015) the cumulative probability becomes:

$$H(x) = q + (1-q)\cdot G(x) \quad (8)$$

where q is the probability of precipitation=0. H(x) is then transformed to the standard normal random variable Z, with zero average and variance equals to one, which becomes the value of the SPI.

$$\boldsymbol{z = SPI = \left(t - \frac{c_0+C_1t+C_2t}{1+d_1t+d_2t_3^2+d_3t^3}\right)} \text{ for, } 0<H(x)<0.5 \quad (9)$$

$$z = SPI = \left(t - \frac{c_0+C_1t+C_2t}{1+d_1t+d_2t_3^2+d_3t^3}\right) \text{for,} 0.5<H(x)<1.0 \quad (10)$$

where,

$$t = \sqrt{ln\left(\frac{1}{H(x)^2}\right)}. \quad \text{for ,} 0<H(x)<0.5 \quad (11)$$

And,

$$t = \sqrt{ln\left(\frac{1}{(1-H(x))^2}\right)} \quad (12)$$

where,

$C_0$=2.515,$C_1$=0.80285,$C_2$=0.0103,$d_1$=1.43278, $d_2$=0.18926 and $d_3$=0.00130 (Mishra and Desai 2005)

For future drought assessment, we employed a CMIP5 multi-model ensemble MME; Fig. 2. At each station, all 14 GCMs were evaluated against IMD precipitation using the performance indicators in TABLE 5. Indicator weights were derived independently using the Entropy weight method and the Analytic Hierarchy Process (AHP), then averaged to obtain a composite weight vector (Pomerol et al. 2000; Raju and Kumar 2014). The weighted indicators were supplied to the MCDM ranking schemes (CP, CGT, and TOPSIS) to produce station-wise ranks. The top five models at each station were then combined into an ensemble, and their monthly precipitation was downscaled/bias-adjusted prior to SPI computation.

(i) *Entropy Weight Method (EWM)*- EWM provides objective indicator weights based on the information content (dispersion) of each indicator across models. Indicators with greater differentiation (lower entropy) receive higher weights, reducing subjective bias in weighting. The major benefit of the EWM over other

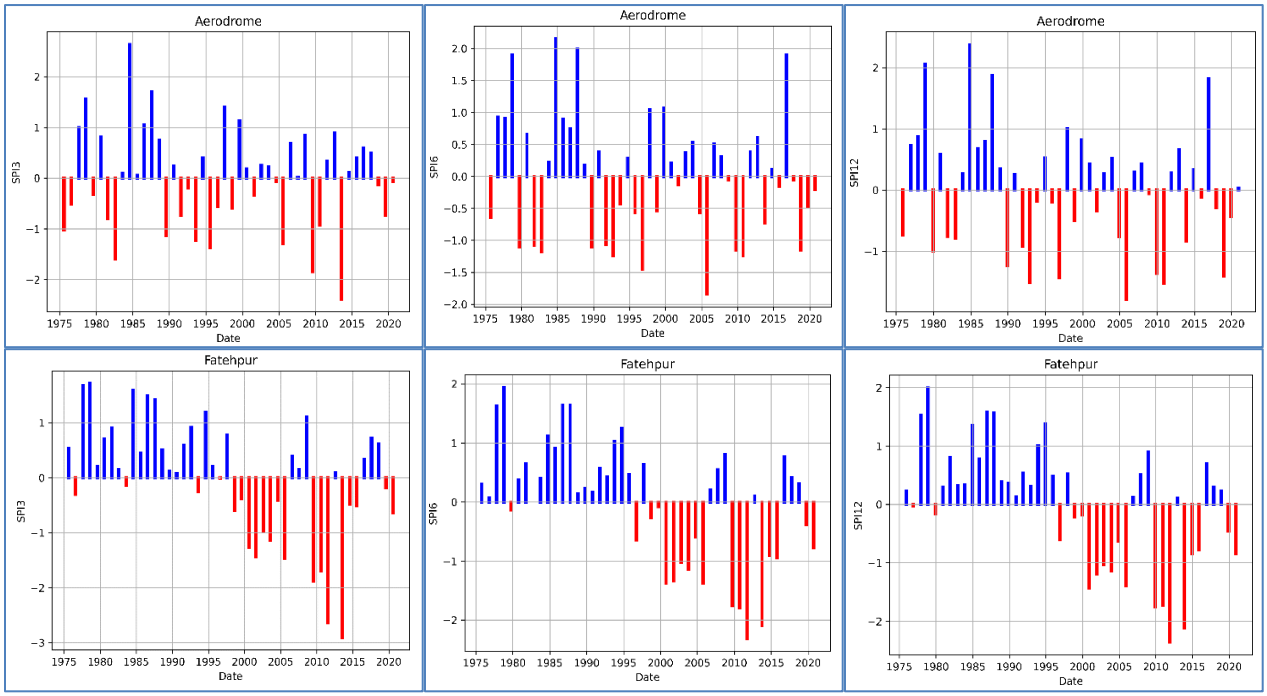


**Fig. 3**. SPI 3, SPI 6, and SPI 12 Plots for Drought prone area for Gaya

subjective weighting models is the elimination of human influence with the weight of indicators, which improves the impartiality of the outcomes of the thorough review. The EWM measures the level of differentiation to assess value. More information can be gleaned from an index whose degree of differentiation is higher than the measured value's degree of dispersion.

(ii) *Analytic Hierarchy Process (AHP):* AHP derives subjective/experiential weights via pairwise comparisons of indicators on a common scale, followed by eigen vector extraction to obtain the priority weights; consistency is checked via the consistency ratio (CR) *Donegan et al. (1992)*. Model performance is then aggregated additively across indicators using these weights. In our workflow, EWM and AHP weights were computed independently and averaged to form a composite weight vector used in subsequent MCDM ranking of the 14 GCMs.

GCM skill was evaluated by comparing simulated precipitation with historical observations (hindcasts), enabling selection of the best-performing models for subsequent analysis (Mujumdar and Kumar 2012). Performance was quantified using eight indicators sum of squares of deviations (SSD), mean square deviation (MSD), root mean square deviation (RMSD), normalized RMSD (NRMSD), absolute normalized mean bias deviation (ANMBD), average absolute relative deviation (AARD), correlation coefficient (CC), and Nash-Sutcliffe efficiency (NSE) with formulas given in TABLE 5.

Station-wise model ranking was then performed using three multi-criteria decision-making (MCDM) methods: compromise programming (CP), cooperative game theory (CGT), and the technique for order preference by similarity to an ideal solution (TOPSIS). The resulting ranks were averaged to obtain a robust overall rank for each GCM at each station.

(1) *Compromise Programming (CP):* - It is established on distance measure Linear Programming (Lp) metric (Raju and Kumar 2014). The GCMs are ranked using compromise programming (CP), a remote decision-making method. The rating patterns derived for individual grid points are combined using a group decision-making approach. Moreover, a straightforward ensemble strategy is recommended.

$$L_{p_a} = \left[\sum_{j=1}^{J} r_j^p \left|k_j^* - k_j \cdot (a)\right|^P\right]^{1/P} \quad (13)$$

where $k_j$ = Value of Indicator j for GCM a; $r_j$ =Weight assigned to the indicator j; P = parameters (1, 2 ….. ∞) also, $k_j^*$ =Ideal value of each indicator j among available.

(2) *Cooperative Game Theory (CGT)*: In the CGT formulation for MCDM, each indicator acts as a "player," and an alternative (here, a GCM) gains payoff according to its closeness to the ideal (and, equivalently, distance from the anti-ideal, i.e., worst observed performance).

After normalizing indicators so that larger is better, the payoff for model $a$ is computed as a weighted distance from the anti-ideal:

$$Da = \pi_{j=1}^{J}.\left|k_j(a)-k_j^{**}\right|^{r\cdot j} \quad (14)$$

For indicators where "smaller is better," the normalization is adjusted accordingly. A higher value of Da indicates that the model is closer to the ideal and farther from the anti-ideal. The models are then ranked in descending order of Da, with higher values indicating better overall performance.

(3) *Technique for Order Preference by Similarity to an Ideal Solution (TOPSIS):* It is a compensatory Multi-Criteria Decision Making (MCDM) method that ranks alternatives based on their proximity to the ideal solution (best performance on every criterion) and distance from the anti-ideal solution (worst performance on every criterion). The process involves the following steps:

(i) *Normalize the Decision Matrix***:** First, normalize the decision matrix. Then, apply the indicator weights rj (from the EWM-AHP average) to obtain the weighted matrix.

(ii) *Define the Ideal and Anti-Ideal Solutions*: Define the ideal solution kj∗ and the anti-ideal solution kj∗∗ for each indicator across all models, using benefit/cost conventions to ensure that all criteria are oriented such that "larger is better."

(iii) Compute Euclidean Distances**:** Calculate the Euclidean distances of model a from both the ideal and anti-ideal solutions:

*Distance from the Ideal Solution:*

$$DS_a^{+} = \sqrt{\sum_{j=1}^{J} r_j\left(K_j(a) - K_j^{*}\right)\text{^}2} \quad (15)$$

where $K_j^{*}$= Ideal values

*Distance from the Anti-Ideal Solution*

$$DS_a^{-} = \sqrt{\sum_{j=1}^{J} r_j\left(K_j(a) - K_j^{**}\right)\text{^}2} \quad (16)$$

And $K_j^{**}$= Anti-ideal value, a is the particular GCM

(iv) *Calculate Relative Closeness to the Ideal*: Further we calculate Relative Closeness $CR_a$

$$CR_a = \frac{DS_a^{-}}{\left(DS_a^{-}+DS_a^{+}\right)} \quad (17)$$

where 0≤ CRa ≤1. A higher value of CRa indicates that the model is closer to the ideal solution.

(v) *Rank the Models:* Finally, rank the models in descending order of Ca, with higher values indicating better performance.

By using TOPSIS alongside CP and CGT methods, we can perform a robustness check on the preference ordering. All methods are supplied with the same averaged weights to obtain consistent station-wise ranks Srinivasa Raju and Nagesh Kumar (2015).

Finally, for better Ranking the ensemble of best five models for each station were used for downscaling the future precipitation data (2021-2050) with the help of a second-degree polynomial fitted between the period (2006-2020) using the least squares regression method. The output values show the acceptable results which can be seen in the further result section.

## 3. Results and discussion

For the preliminary process trend test were done station-wise, i.e TABLE 3 the MK test reveals predominantly negative z-values, indicating declining precipitation at several locations-Rajauli, Chandi, Sikandra, Chakaibanda, Fatehpur, and Aerodrome-with statistically significant trends in multiple cases (*e.g*., Aerodrome: z = −2.53, p = 0.025). These declines are consistent with more frequent dry spells and reduced rainfall intensity, implying heightened meteorological-drought risk. By contrast, Lakhisarai exhibits a positive but non-significant trend, suggesting localized increases insufficient to offset the broader drying signal. The Coexistence of significant and non-significant trends across neighbouring stations highlights strong spatial heterogeneity, likely influenced by topography, microclimates, and land-use change. Overall, the pattern underscores South Bihar's vulnerability to shifting precipitation regimes and signals early warning signs of long-term water stress.

### 3.1. *Historical analysis using SPI*

Historical SPI (1975–2020) computed from IMD station data shows notable shifts in drought occurrence across Gaya, Jamui, Lakhisarai, Nalanda, and Nawada. Fig. 3 to Fig. 8 present SPI time series for all ten stations. At many stations, events with SPI ≤ −1.5 at 6- and 12-month scales have become more frequent after 2000, indicating a shift from moderate to severe-and occasionally extreme drought conditions. Across several districts, the share of drought years increased by roughly 10-30% (station-dependent).

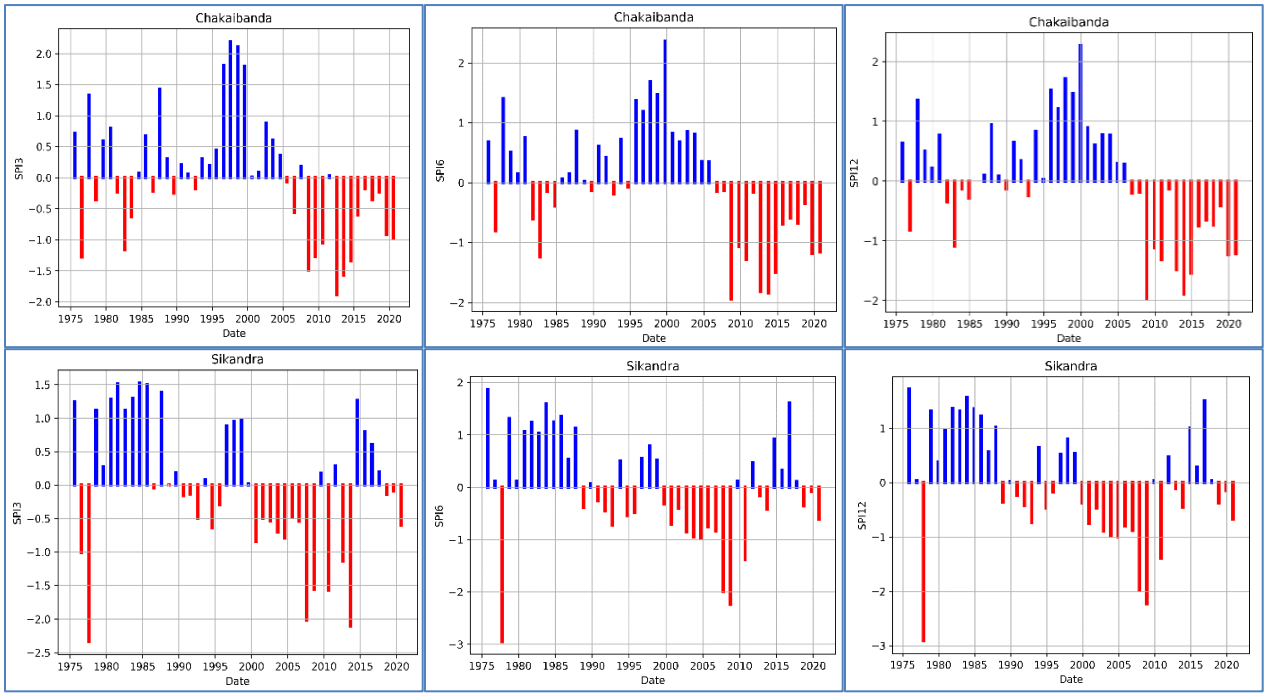


**Fig. 4.** SPI Plots for the Drought Prone area for Jamui

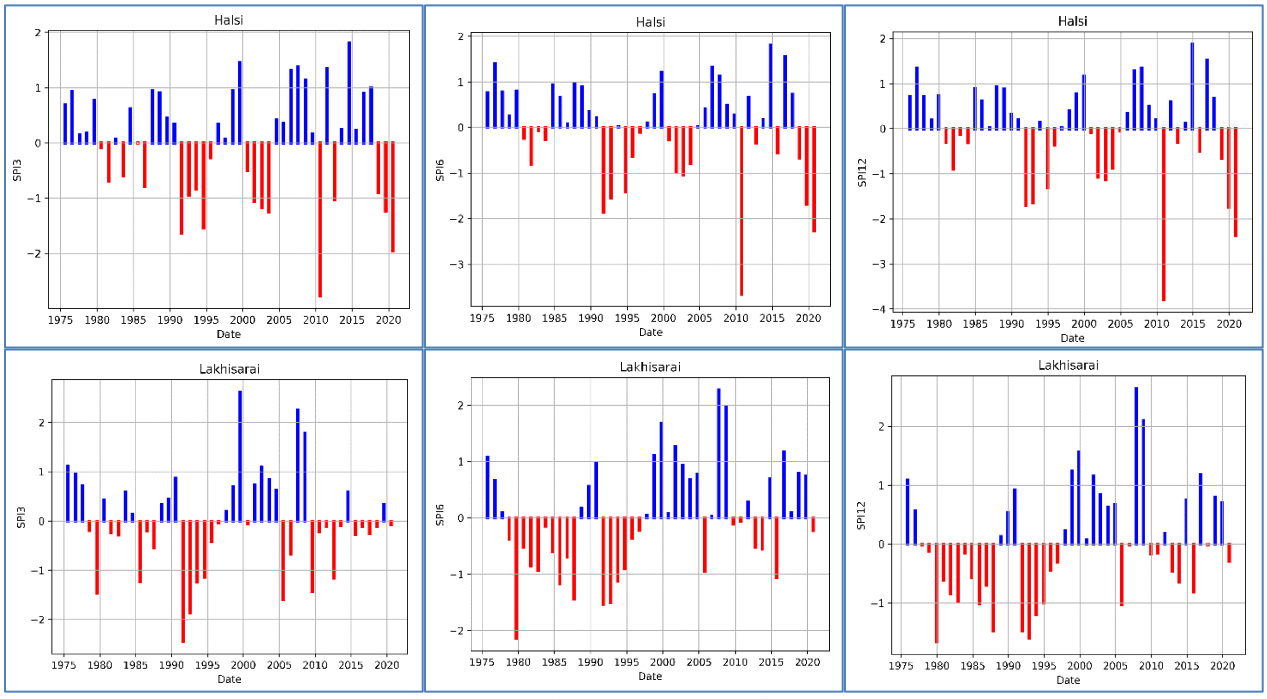


**Fig. 5.** SPI Plots for Drought prone area of Lakhisarai

Fig. 3 shows SPI at 1-, 6-, and 12-month scales for Aerodrome (top row) and Fatehpur (bottom row) during 1975–2020. At Aerodrome, negative anomalies intensify after ~2000: events with SPI $\leq -1.5$ occur more often at SPI-6 and SPI-12, with clusters around 2002–2009 and 2014–2020, while strong positive spikes common in the 1980s–1990s become infrequent and weaker. Fatehpur exhibits a stronger drying signal: since ~2000 the SPI-6/-12 series are predominantly negative, including several extreme events (SPI $\leq -2$), indicating persistent multi-month moisture deficits. The SPI-1 series at both stations remains more variable year-to-year, but dry Junes become

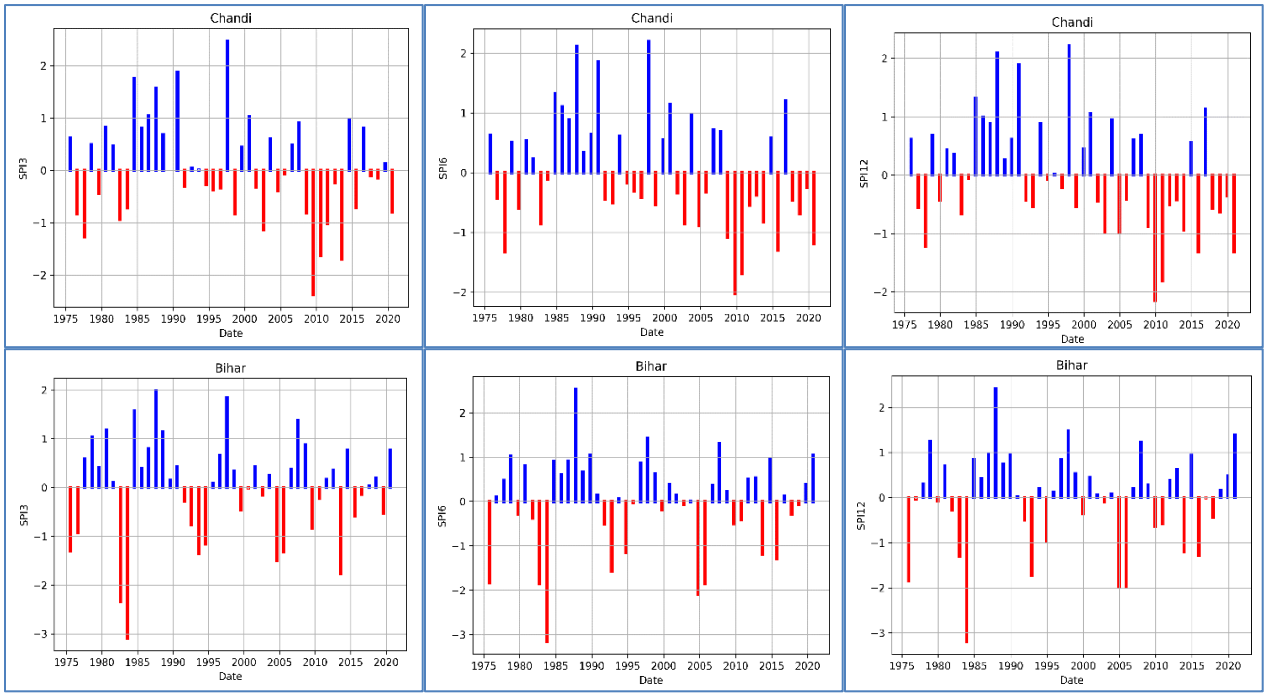


**Fig. 6.** SPI plots for drought prone area for Nalanda

noticeably more frequent after 2000. Together, these patterns indicate a shift from episodic wet–dry fluctuations to more sustained drought conditions in the later decades, particularly at Fatehpur.

The Jamui stations show a clear post-2000 shift toward drier conditions. Chakaibanda is predominantly wet through the 1980s–mid-1990s, but after ~2000 the SPI-6/-12 series turn negative more frequently, with several severe (SPI ≤ −1.5) and occasional extreme (SPI ≤ −2) events during the 2010s; SPI-1 remains noisy, yet dry Junes become more common after 2005. Sikandra exhibits a stronger and more persistent drying signal: SPI-6 and SPI-12 are largely negative from the late 1990s onward, punctuated by multiple severe-to-extreme episodes, indicating sustained multi-season to multi-annual moisture deficits. Overall, the records indicate a transition from episodic wet–dry variability to sustained drought propensity in Jamui after 2000, with Sikandra being the most affected.

Fig. 5 & Fig. 6 summarizes SPI at 3-, 6-, and 12-month scales for Halsi (Lakhisarai) and Chandi (Nalanda) during 1975–2020. At Halsi, negative anomalies become more frequent after ~2000, with several severe events (SPI ≤ −1.5) at SPI-6/-12, especially post-2010, indicating persistent multi-season moisture deficits; pre-2000 records show a more balanced mix of wet and dry years. Chandi exhibits a similar evolution, with extended dry spells in the early 2000s and again after 2010, and SPI-6/-12 remaining negative for long stretches, consistent with long-term drought conditions. Positive SPI values before 2000-mark wetter intervals at both stations. Overall, both locations show a shift in the last two decades from episodic variability to sustained drought propensity, underscoring increasing aridity and hydroclimatic variability in South Bihar.

The drought episodes in the Lakhisarai district state that both Halsi and Lakhisarai stations indicate a higher incidence of severe to extreme drought events for SPI 6 and SPI 12 between 1990 to 1995, mainly for Lakhisarai stations. Similarly, in the Nalanda district, Chandi and Bihar stations were analyzed, with Chandi exhibiting more frequent drought events after 2000 for both SPI 6 and SPI 12. Additionally, for the Nawada district, the stations Nawada and Rajauli were studied, with Rajauli demonstrating a greater occurrence of drought events between 2000 to 2015 across different SPI timescales.

Fig. 8 illustrates that stations such as Aerodrome, Chakaibanda, Halsi, and Lakhisarai depict severe drought conditions for SPI 1 during the month of June.

A short-term dryness is provided by SPI 1 (1-Month *i.e* June month) and SPI 3 (3-Month, *i.e* June-august), which highlights sensitivity to abrupt changes in precipitation and suitability for monthly and seasonal assessments. Here we can see there is not much significant dryness observed in the short-term Drought index. On the

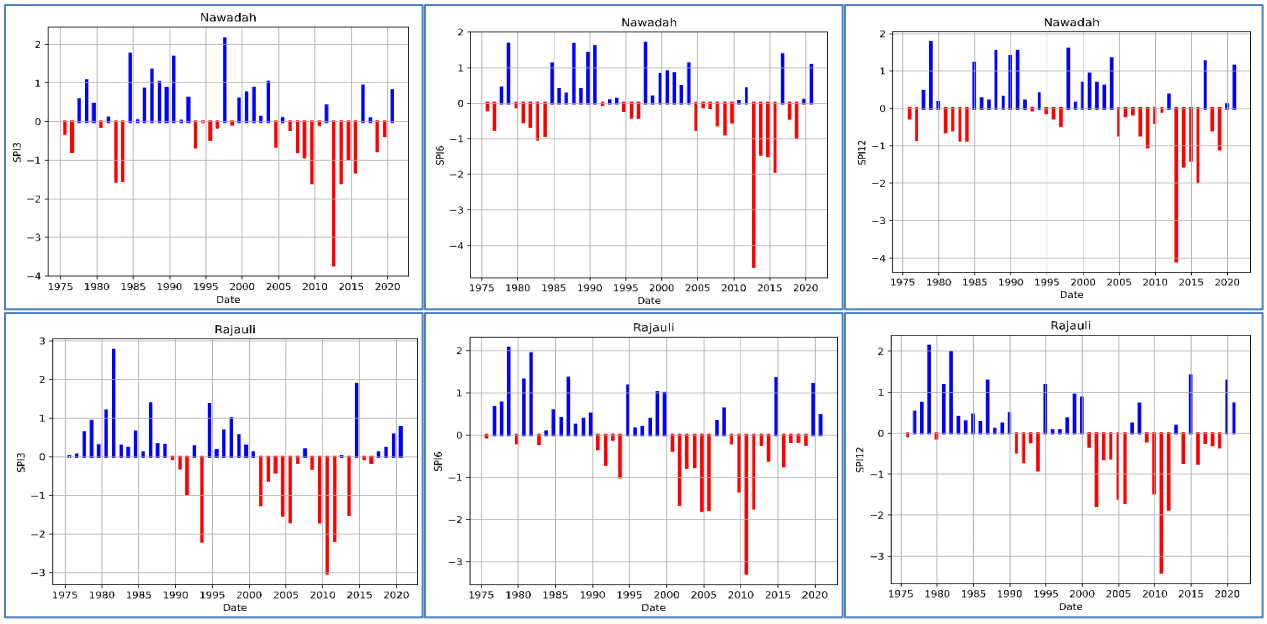


**Fig. 7.** SPI plots for drought prone area for Nawada

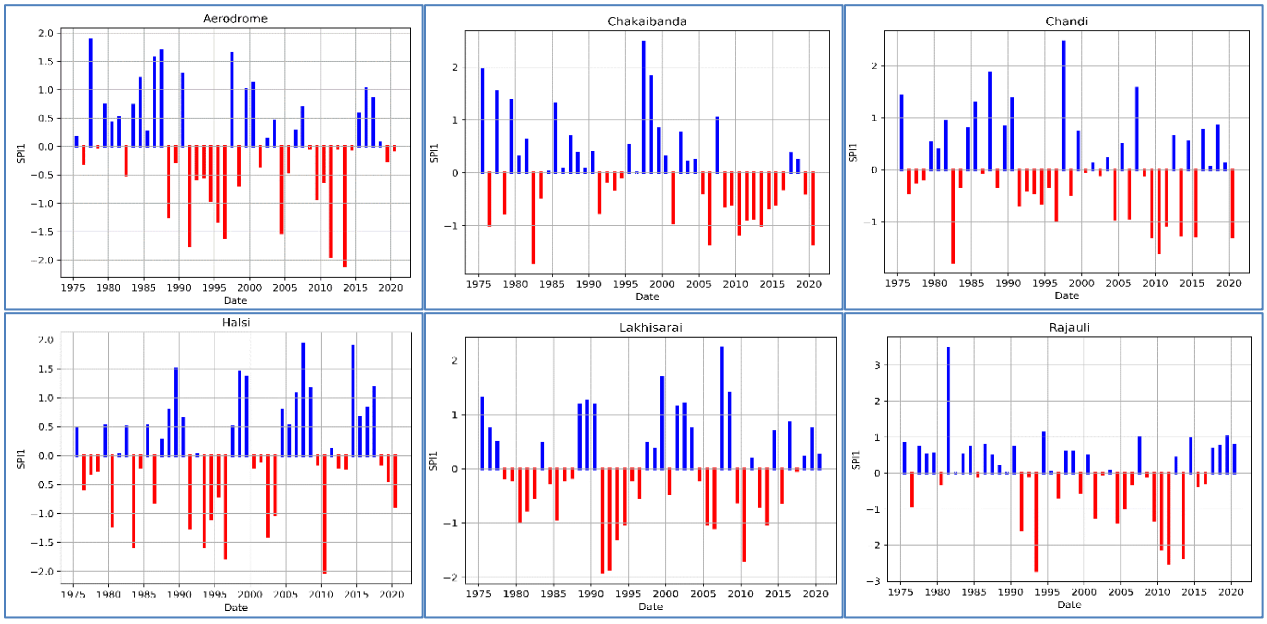


**Fig. 8.** SPI 1 Plots for Some Meteorological stations

other hand, SPI 6 (6-Month i.e. June-November) and SPI 12 (12-Month i.e. Jan-Dec) focus on more consistent views across half-year and annual intervals while balancing short-term unpredictability.

### 3.2. *Ranking of CMIP5 GCMs model and Determination of Most suitable GCM for the Study Area*

Performance indicators and their weights (Entropy and AHP) are provided in the Supplementary Material. Fig. 9 shows boxplots of station-wise averaged ranks obtained from three MCDM methods CP, CGT, and TOPSIS and their arithmetic mean. Across the 14 GCMs, the top five are HadGEM2-AO, MRI-CGCM3, MIROC5, CESM1-CAM5**,** and CCSM4; MRI-CGCM3 and HadGEM2-AO most consistently rank highest, whereas GISS-E2-H and IPSL-CM5A-MR rank lowest. Notably, IPSL-CM5A-MR shows a narrow interquartile range (low variability) yet a poor median rank stability does not imply skill while CESM1-CAM5 and MIROC-ESM exhibit wider spreads, indicating sensitivity to method and

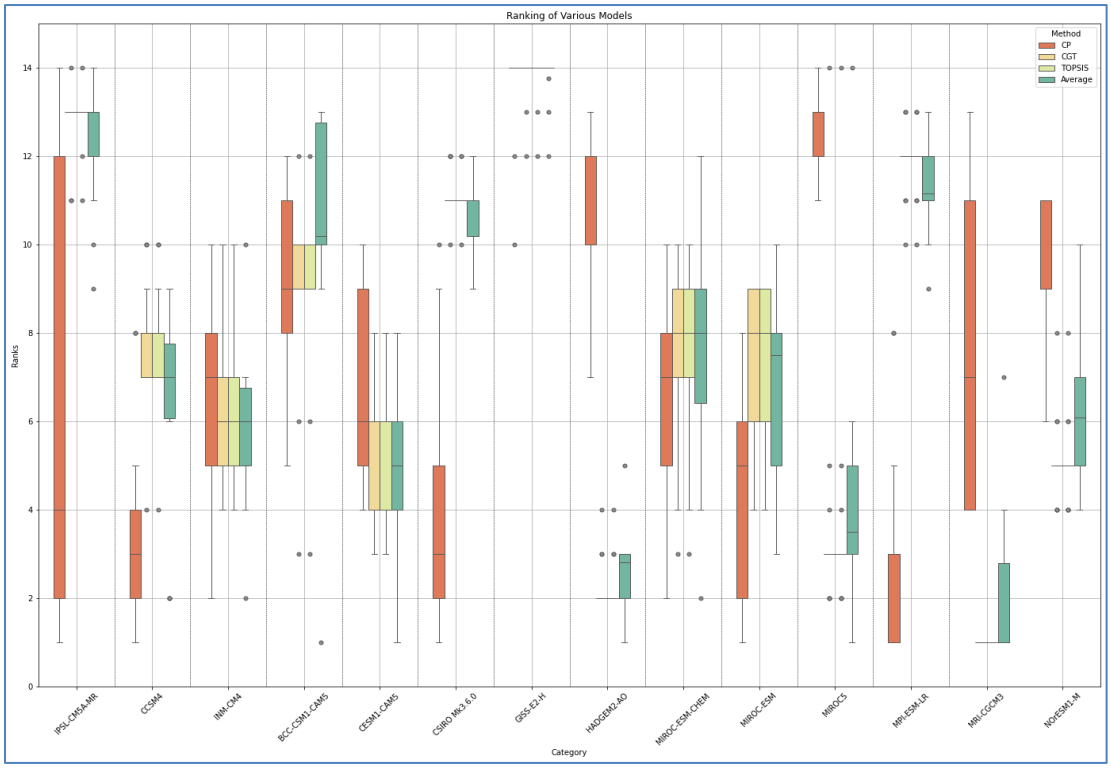


**Fig. 9.** Box Plot of all three MCDM techniques and average Ranking

station. Rank disparities among CP, CGT, and TOPSIS (including outliers) underscore the value of a multi-criteria approach. Accordingly, the top five models at each station were selected to construct the ensemble used for downscaling and subsequent SPI analysis.

### 3.3. *Downscaling of GCMs simulated data*

After identifying the top five GCMs at each station, we formed an ensemble and applied a second-degree polynomial bias - correction/ downscaling between simulated and observed precipitation. ensemble models, a critical step in refining precipitation predictions involves the application of a second-degree polynomial regression model. This model, represented as $\boldsymbol{y = Ax^2 + Bx + C}$, captures the relationship between the General Circulation Model (GCM) simulated precipitation ($\boldsymbol{x}$) and the observed Indian Meteorological Department (IMD) data ($\mathbf{y}$) for each specific station. The coefficients A, B, and C are determined through the least square's regression method, optimizing the fit of the polynomial curve to the historical data. With the established regression model, projections for precipitation over each station are made for the upcoming years from 2021 to 2050. The polynomial equation enables a nuanced understanding of the simulated versus observed precipitation trends, accounting for the complex interplay between variables. The precision of the second-degree polynomial regression model allows for a more accurate representation of potential shifts in rainfall, providing decision-makers with actionable information to address evolving climate conditions.

By applying this methodology across various stations, researchers and policymakers gain a comprehensive view of regional precipitation forecasts, facilitating proactive measures to mitigate the impact of changing climatic conditions on local ecosystems, agriculture, and water availability. The integration of ensemble models and polynomial regression enhances the robustness of climate predictions, contributing to a more resilient and adaptive approach in the face of ongoing environmental changes.

### 3.4. *Validation of GCM predicted rainfall*

The predicted values from the previous step are validated with observed IMD data. Fig. 10 to Fig. 14 shows the time series plots of GCM simulated (ensemble) and IMD observed rainfall data at monthly timescale. The results indicate a good match of GCM simulated precipitation with IMD observed data. The variability is well captured but the peaks are underestimated by the GCMs. This can be attributed to the coarse resolution of the GCM data.

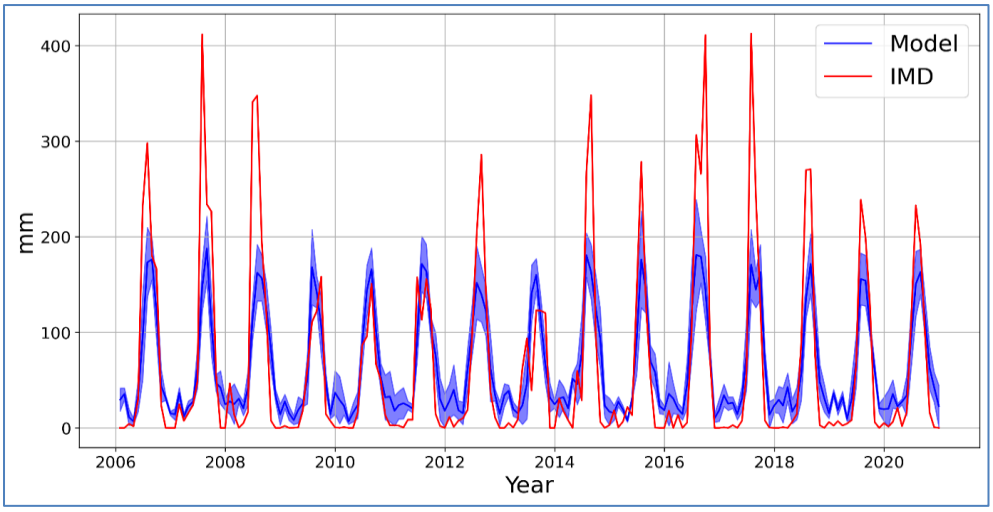


**Fig. 10.** Time series plots for IMD versus GCMs model (2006-2020) for Gaya

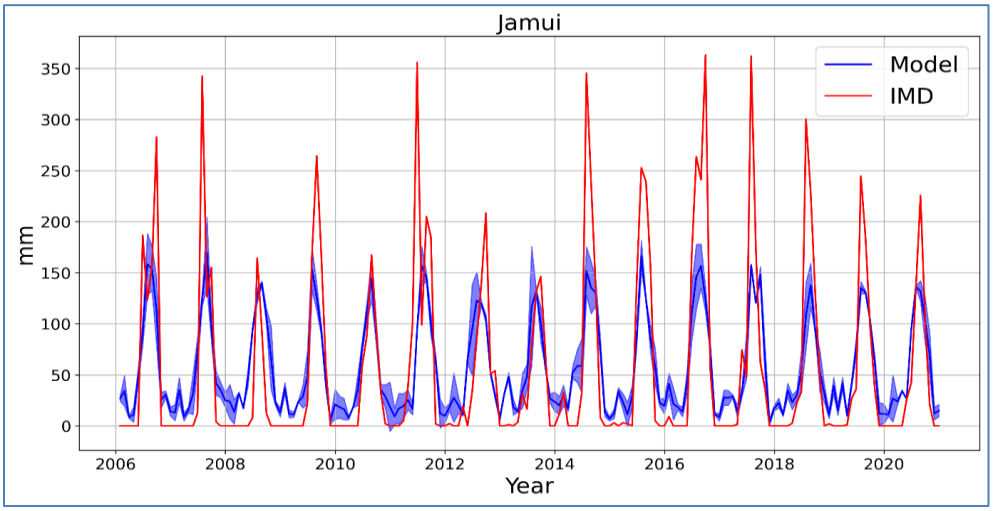


**Fig. 11.** Time series plots for IMD versus GCMs model (2006-2020) for Jamui district

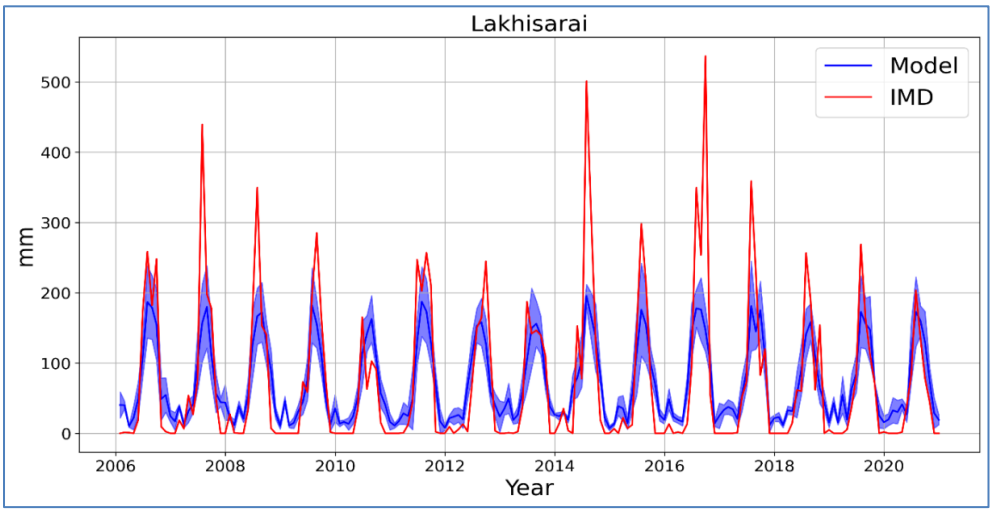


**Fig. 12.** Time Series plots for IMD versus GCMs model (2006-2020) for Lakhisarai district

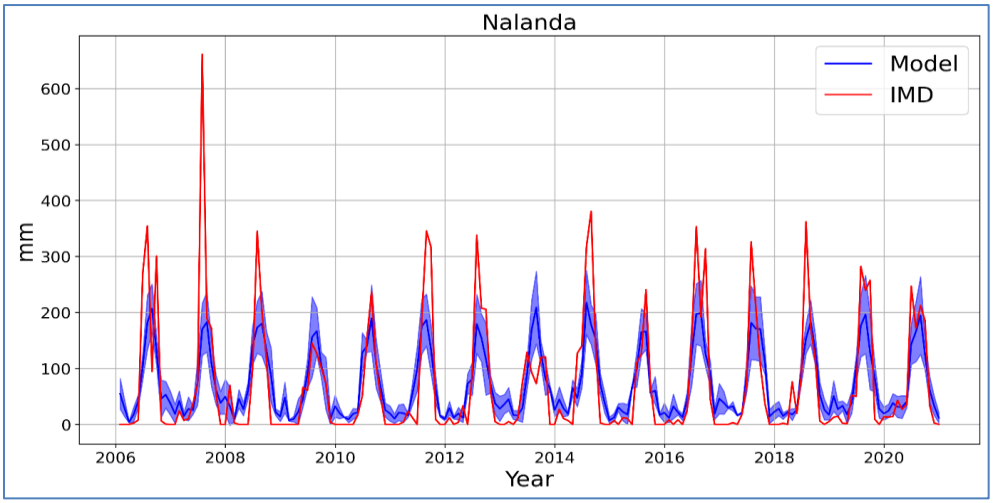


**Fig. 13.** Time Series plots for IMD versus GCMs model (2006-2020) for Nalanda district

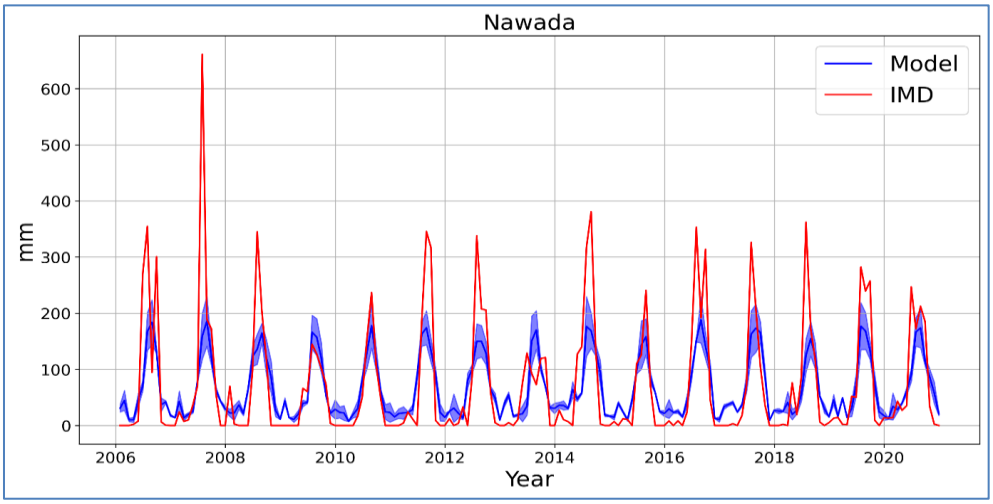


**Fig. 14.** Time series plots for IMD versus GCMs model (2006-2020) for Nawada

The shaded area illustrates the range of variability among simulated model outputs, presenting time series comparisons of precipitation data from the Indian Meteorological Department (IMD) alongside simulated data from the General Circulation Model (GCM). These figures surely representing us the both data have strong correlation.

For Lakhisarai and Nalanda (2006–2020), the downscaled GCM ensemble closely tracks IMD monthly seasonality and interannual variability, indicating strong agreement. Peak rainfall, however, is systematically underestimated IMD extremes exceed the ensemble. The blue-shaded band marks the ensemble spread; most observations fall within this range, supporting overall skill. Nonetheless, the attenuation of extremes suggests scope for refinement (*e.g.*, variance/quantile-based bias correction or higher-resolution inputs) to better capture heavy-rainfall events.

The scatter plots depicting the relationship between the observed IMD (x-axis) and predicted GCM model (y-axis) precipitation are presented in Fig. 15. The analysis reveals a strong correlation between the predicted and observed precipitation values, with $R^2$ values ranging from 0.628 to 0.732. Notably, the highest $R^2$ value of 0.732 was recorded at the Gaya station, indicating a robust fit between the observed and modelled data. In contrast, Nawada exhibited the lowest $R^2$ value of 0.628, suggesting a slightly weaker correlation. The results for other stations Lakhisarai ($R^2$ = 0.716), Jamui ($R^2$ = 0.663), and Nalanda ($R^2$ = 0.656) demonstrated generally acceptable levels of model performance. These findings suggest that the GCM model provides a reliable

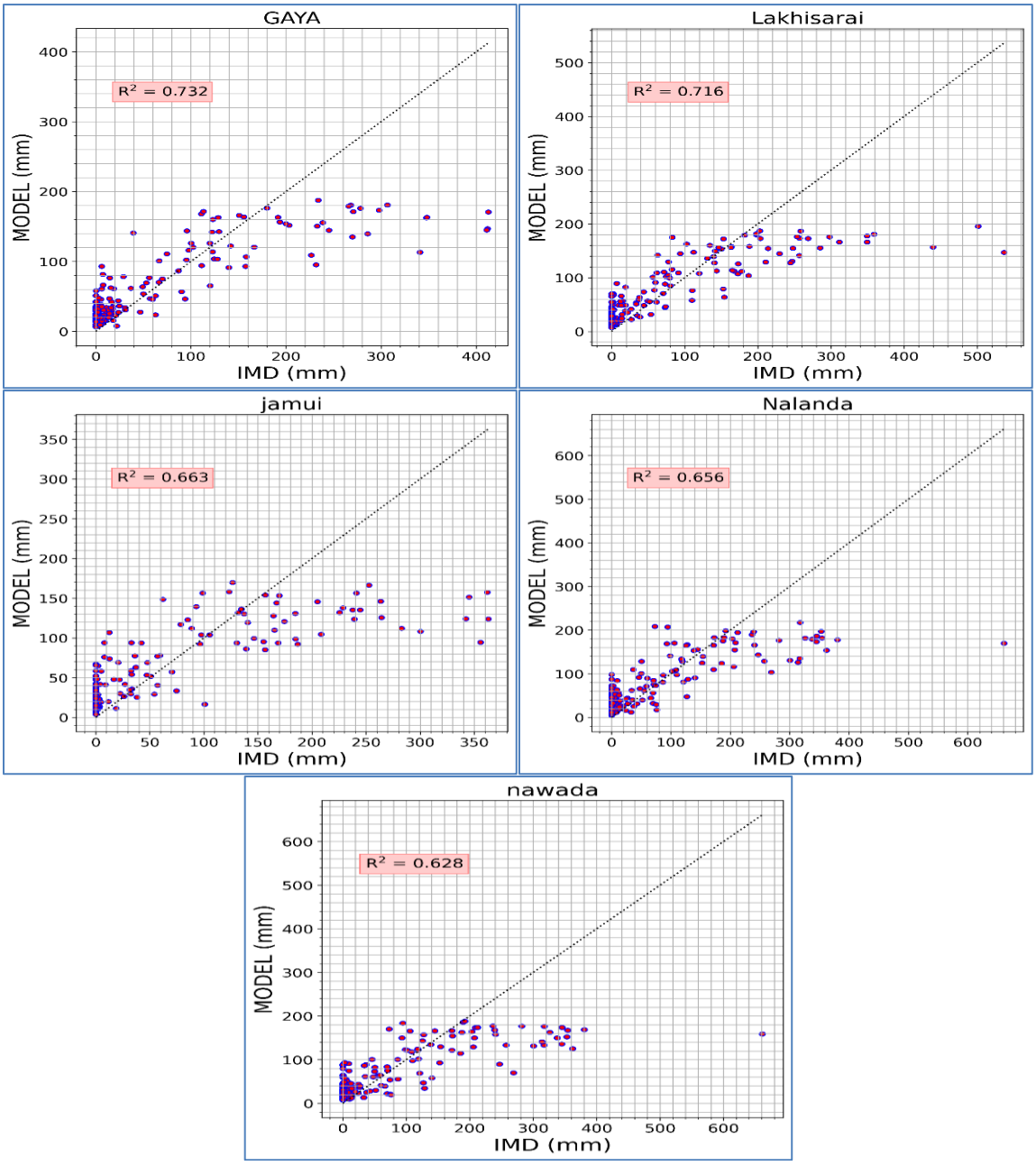


**Fig. 15**. PLOT OF IMD VS GCMs MODEL Scatter

approximation of observed precipitation, particularly in regions like Gaya and Lakhisarai, where the highest $R^2$ values were observed. The scatter plots for all districts, including Nawada, Jamui, and Nalanda, are presented in accordance with the reviewer's request, further supporting the consistency of the model across different regions.

### 3.5. *Future drought analysis using SPI*

The future analysis of SPI values, derived from the precipitation data of GCMs simulated output spanning the period 2021-2050, reveals noteworthy trends in drought occurrences across several districts in different timescales, mainly in Gaya Jamui, Lakhisarai Nalanda and Nawada. Fig. 16 to Fig. 20 depict the SPI plots derived from simulated future data using GCMs models spanning the timeframe from 2021 to 2050.

Examining the various time scales, SPI reveals a constant trend in wetness after 2040. This could be attributable to enhanced moisture convergence and also increased convective activity caused by accelerated global

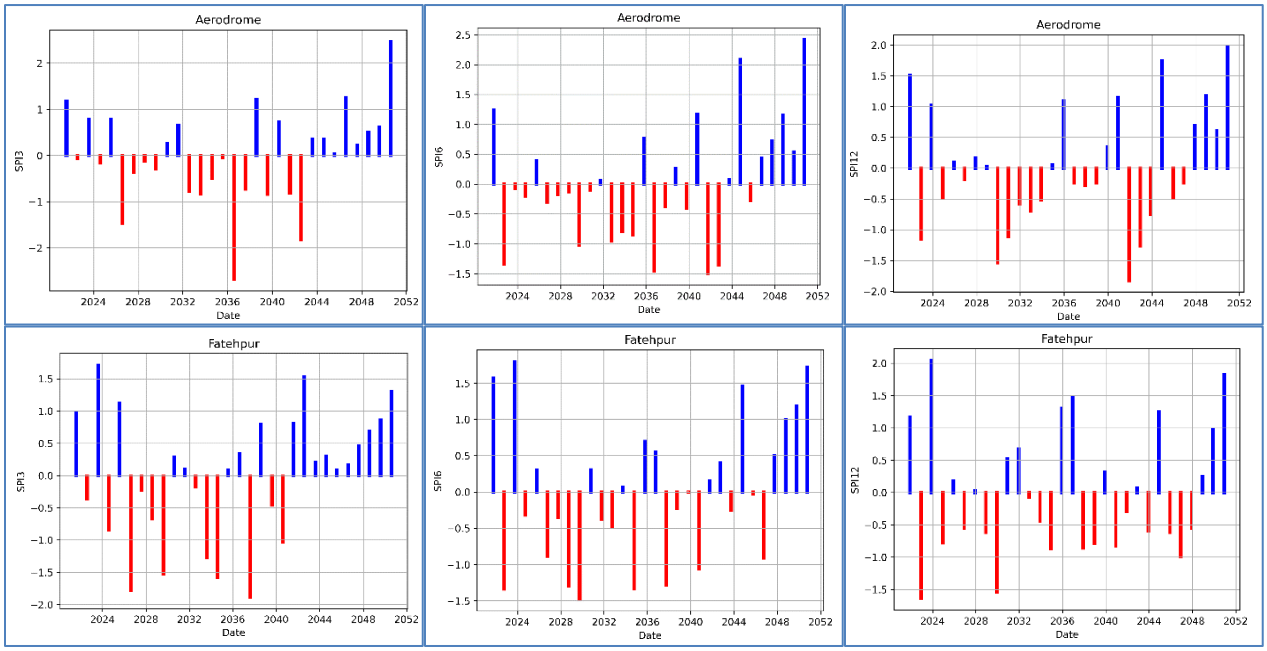


**Fig. 16.** Future SPI 3, SPI 6, and SPI 12 Plots for Gaya Districts

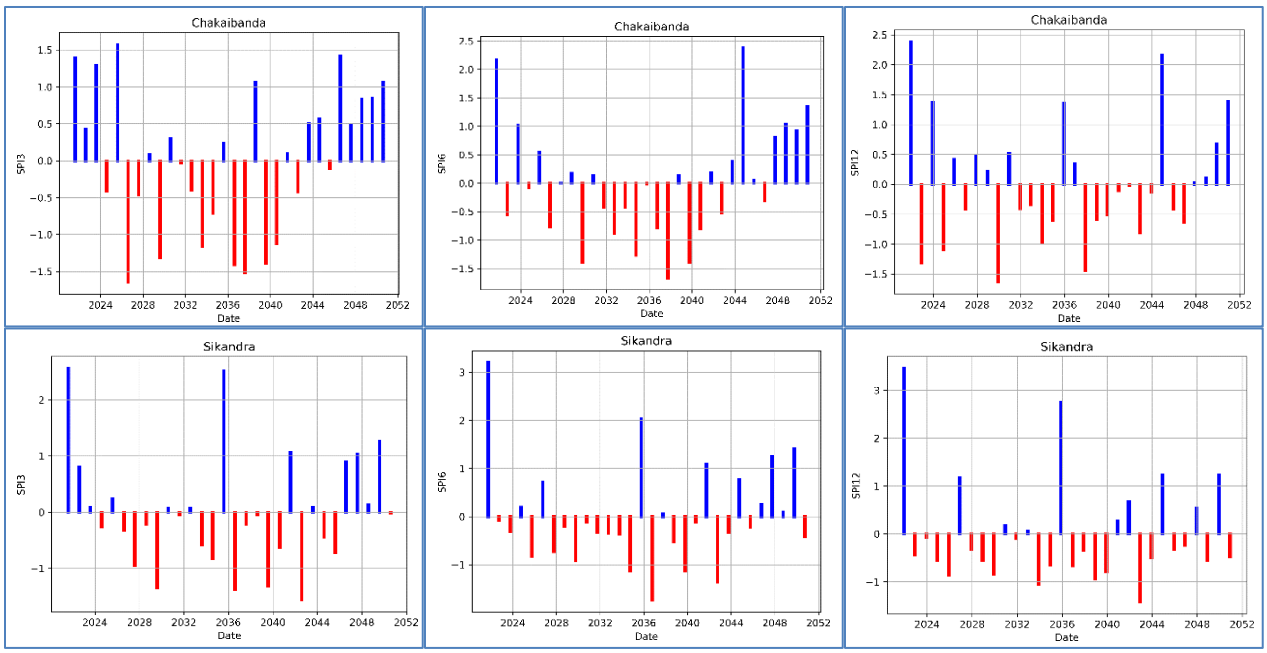


**Fig. 17.** SPI 3, SPI 6, and SPI 12 Plots for Jamui Districts

warming and related feedback mechanisms, as simulated by CMIP5 models.

The future Standardized Precipitation Index (SPI) for both Aerodrome and Fatehpur indicates a rise in precipitation variability. The SPI3, SPI6, and SPI12 values reflect periods of long-term drought (negative SPI, shown in red) and excessive rainfall (positive SPI, shown in blue). In Aerodrome, extreme positive SPI values are observed after 2040, with a peak around 2050, suggesting a transition towards drier conditions. However, intermittent periods of drought persist in the later years. In Fatehpur, droughts become progressively severe until 2040, after which the region experiences drier conditions in subsequent years. This pattern, with fluctuations between drought and rainfall, suggests significant climate

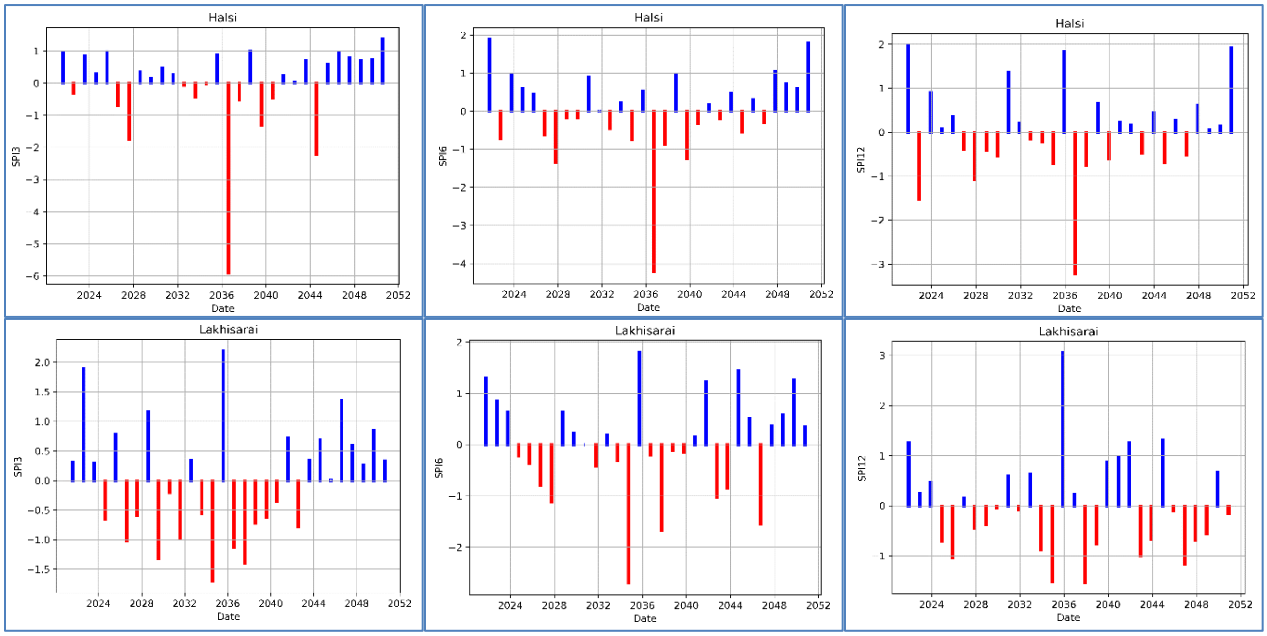


**Fig. 18.** SPI 3, SPI 6 and SPI 12 Plots for Lakhisarai Districts

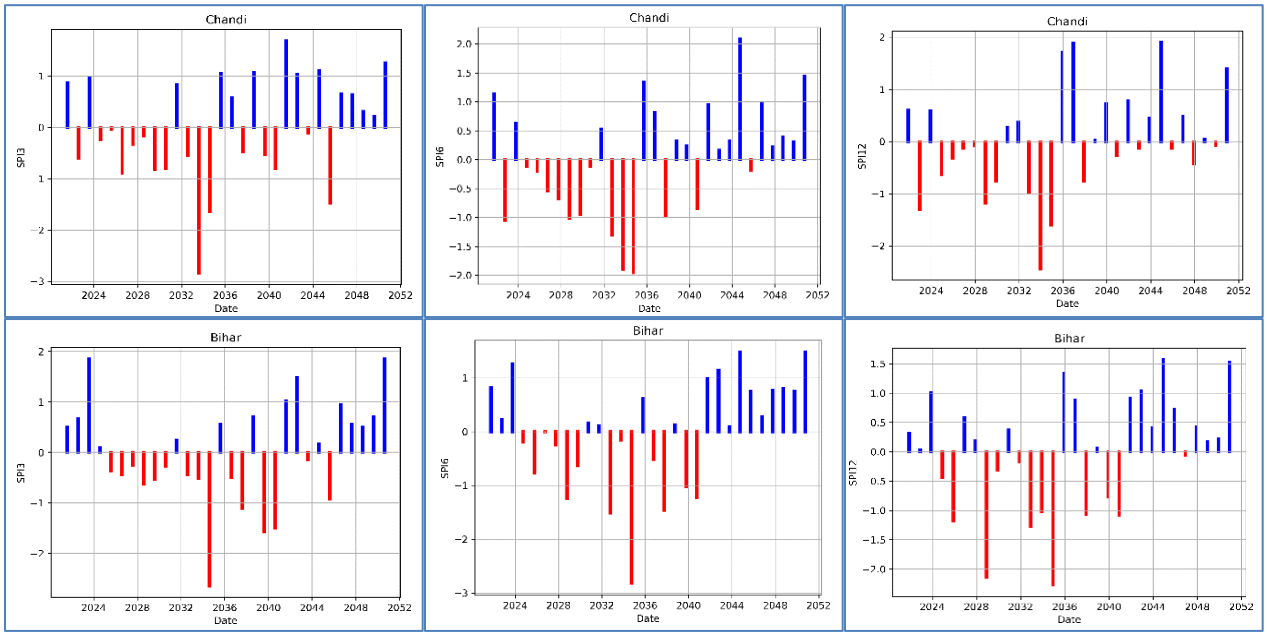


**Fig. 19.** SPI 3, SPI 6, and SPI 12 Plots for Nalanda Districts

variability for both locations. The alternating wet and dry periods indicate that both areas will likely face more frequent extreme weather events. Therefore, adaptive water resource management strategies should be considered to mitigate the effects of drought and leverage drier periods for sustainable development.

In the Gaya district, stations like Aerodrome and Fatehpur show an increased frequency of drought occurrences. SPI6 and SPI12 data for Aerodrome indicate an escalation in drought events post-2030, while Fatehpur experiences an increase in drought cases from SPI3 and SPI6 until 2040, followed by a shift towards wetter conditions thereafter. Similarly, in the Jamui district, the Chakaibanda station exhibits severe to extreme drought conditions for SPI3 and SPI6 between 2030 and 2040, transitioning to wetter conditions afterward. In Jamui, stations, such as Sikandra showcase persistent dryness during the monsoon period from 2030 until 2040.

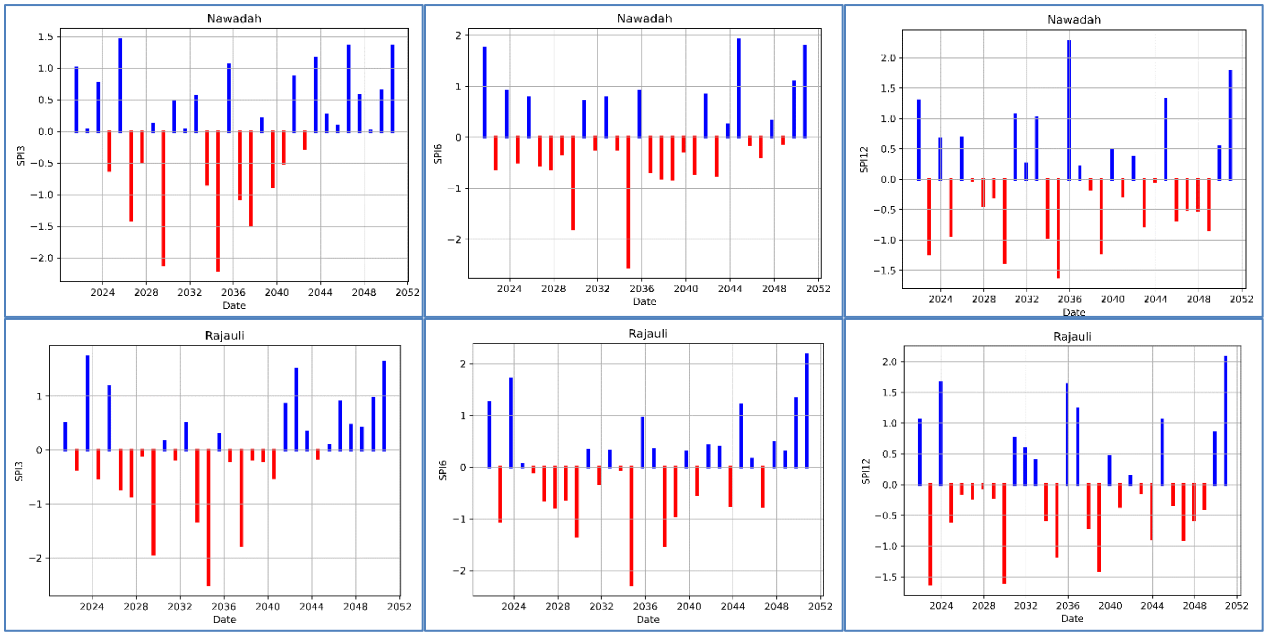


**Fig. 20.** SPI 3, SPI 6, and SPI 12 PLOTs for Nawada Districts

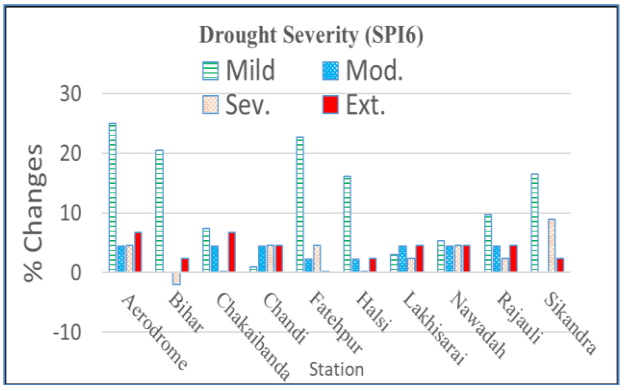


**Fig. 21**. Drought percentages mild moderate and severe for SPI6

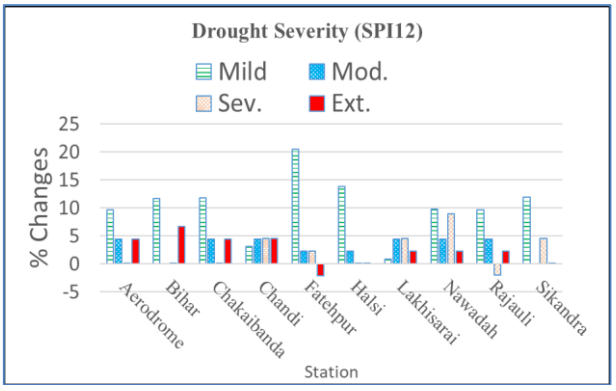


**Fig. 22.** Drought Percentages change for mild, moderate-severe, and extreme cases (SPI12)

In the Lakhisarai district, Halsi experienced extreme drought cases between 2030 and 2040, while Lakhisarai station shows consistent dryness, particularly in the monsoon season, as evidenced by SPI 3 data. The trends in Nalanda district stations, Chandi and Bihar, mirror those observed in Gaya and Jamui, with severe drought prevalent between 2030 to 2040 across different SPI timescales, followed by a shift towards wetter conditions after 2040. Finally, in the Nawada district, stations like Nawada and Rajauli initially exhibit dry SPI periods from 2030 to 2040, followed by wetter periods thereafter.

### 3.6. *Effect of Climate change on Drought indices*

Using the predicted precipitation data for the period 2021-2050, the future SPI6 and SPI12 were estimated and compared with the past SPI indices as shown in TABLE 6& TABLE 7 as well as in Figs. 21 and Fig. 22. Here TABLE 6 droughts (*i.e*. mild, moderate, severe, and extreme) for Historical and Predicted scenarios for all ten stations. During the historical time, on average there were nearly 20-40% mild cases,10-20% moderate and 5 to 10 % severe to extreme cases, which changed to about 40-60% mild, 10-15 % Moderate. Although there is an average increase in mild cases, Chandi station, shows a drop in mild cases, whereas these cases have nearly doubled in Aerodrome , Bihar, Fatehpur, and Halsi stations Similarly, for the moderate cases, four stations, Bihar, Chandi, Nawada, Rajauli show significant increase in severe drought cases.

Analysis of future climate scenarios reveals that even the most conservative projections, derived from the

**TABLE 6**

**Percentage of drought severity for IMD Individual Meteorological stations**

| %age Change | | SPI6 | | | | | | | | | | | |
|---|---|---|---|---|---|---|---|---|---|---|---|---|---|
| | | Historical (1975-2020) | | | | Predicted (2021-2050) | | | | | | | |
| | | Mild | Mode-rate | Severe | Extreme | Mild | | Moderate | | Severe | | Extreme | |
| S. No | Station | | | | | Min | Max | Min | Max | Min | Max | Min | Max |
| 1 | Aerodrome | 26.09 | 21.74 | 2.17 | 0.00 | 28.89 | 51.11 | 4.44 | 8.89 | 0.00 | 6.67 | 0.00 | 6.67 |
| 2 | Bihar | 21.74 | 6.52 | 8.70 | 4.35 | 17.78 | 42.22 | 0.00 | 13.33 | 2.22 | 6.67 | 2.22 | 6.67 |
| 3 | Chakaibanda | 30.43 | 10.87 | 6.52 | 0.00 | 33.33 | 37.78 | 4.44 | 6.67 | 0.00 | 6.67 | 0.00 | 6.67 |
| 4 | Chandi | 43.48 | 8.70 | 2.17 | 2.17 | 22.22 | 44.44 | 4.44 | 17.78 | 2.22 | 6.67 | 0.00 | 6.67 |
| 5 | Fatehpur | 19.57 | 10.87 | 4.35 | 4.35 | 35.56 | 42.22 | 2.22 | 6.67 | 4.44 | 8.89 | 0.00 | 4.44 |
| 6 | Halsi | 23.91 | 4.35 | 6.52 | 4.35 | 15.56 | 40.00 | 2.22 | 6.67 | 0.00 | 6.67 | 0.00 | 6.67 |
| 7 | Lakhisarai | 34.78 | 8.70 | 4.35 | 2.17 | 28.89 | 37.78 | 4.44 | 11.11 | 0.00 | 6.67 | 0.00 | 6.67 |
| 8 | Nawada | 39.13 | 6.52 | 2.17 | 2.17 | 26.67 | 44.44 | 4.44 | 13.33 | 0.00 | 6.67 | 0.00 | 6.67 |
| 9 | Rajauli | 34.78 | 2.17 | 8.70 | 2.17 | 24.44 | 44.44 | 4.44 | 6.67 | 0.00 | 11.11 | 0.00 | 6.67 |
| 10 | Sikandra | 41.30 | 2.17 | 2.17 | 4.35 | 33.33 | 57.78 | 0.00 | 6.67 | 0.00 | 11.11 | 0.00 | 6.67 |

**TABLE 7**

**Percentage of Drought severity for IMD Individual Meteorological Station**

| % Change | | SPI12 | | | | | | | | | | | |
|---|---|---|---|---|---|---|---|---|---|---|---|---|---|
| | | Historical (1975-2020) | | | | Predicted (2021-2050) | | | | | | | |
| | | Mild | Mode-rate | Severe | Extreme | Mild | | Moderate | | Severe | | Extreme | |
| S. No | Station | | | | | Min | Max | Min | Max | Min | Max | Min | Max |
| 1 | Aerodrome | 32.61 | 8.70 | 6.52 | 0.00 | 24.44 | 42.22 | 2.22 | 11.11 | 2.22 | 6.67 | 0.00 | 4.44 |
| 2 | Bihar | 23.91 | 6.52 | 6.52 | 2.17 | 24.44 | 35.56 | 2.22 | 11.11 | 2.22 | 6.67 | 0.00 | 8.89 |
| 3 | Chakaibanda | 28.26 | 13.04 | 6.52 | 0.00 | 28.89 | 40.00 | 2.22 | 11.11 | 4.44 | 6.67 | 0.00 | 4.44 |
| 4 | Chandi | 41.30 | 6.52 | 2.17 | 2.17 | 26.67 | 44.44 | 2.22 | 11.11 | 0.00 | 6.67 | 0.00 | 6.67 |
| 5 | Fatehpur | 21.74 | 10.87 | 4.35 | 4.35 | 24.44 | 42.22 | 2.22 | 20.00 | 2.22 | 6.67 | 0.00 | 2.22 |
| 6 | Halsi | 23.91 | 6.52 | 6.52 | 4.35 | 20.00 | 37.78 | 2.22 | 15.56 | 0.00 | 6.67 | 0.00 | 4.44 |
| 7 | Lakhisarai | 39.13 | 10.87 | 4.35 | 0.00 | 24.44 | 40.00 | 6.67 | 17.78 | 2.22 | 8.89 | 0.00 | 2.22 |
| 8 | Nawada | 36.96 | 6.52 | 4.35 | 2.17 | 22.22 | 46.67 | 6.67 | 15.56 | 0.00 | 13.33 | 0.00 | 4.44 |
| 9 | Rajauli | 32.61 | 2.17 | 8.70 | 2.17 | 31.11 | 42.22 | 4.44 | 11.11 | 2.22 | 6.67 | 0.00 | 4.44 |
| 10 | Sikandra | 36.96 | 4.35 | 2.17 | 4.35 | 33.33 | 48.89 | 4.44 | 13.33 | 0.00 | 6.67 | 0.00 | 4.44 |

minimum values of the five best-performing climate models, indicate a significant increase in severe and extreme weather events across numerous stations, with notable occurrences projected for Aerodrome, Chakaibanda, Chandi, Lakhisarai, Nawada, and Rajauli.

In the TABLE 7 analysing the values for historical and predicted conditions across various stations reveals predominantly mild deviations from the long-term average precipitation. For instance, at Aerodrome, the historical Percentage drought indicates a wet condition, constituting 32.61% above the average, while the predicted suggests a deviation of 42.22 %. Similarly, stations like Fatehpur, and Halsi, shows almost double change in predicted years. For moderate drought significant change can be seen over Bihar,Chandi, Fatehpur, Halsi, Nawada, and Sikandra stations up to 10-15% except Chakaibanda shows decrease in moderate drought. Severe to extreme droughts are observed at most stations, except at Fatehpur, Halsi and, and Sikandra.

The percentage changes indicate departures from the long-term average, but the overall pattern suggests

relatively stable conditions with only minor variations in precipitation levels expected over the next 12 months across these locations.

The above two drought severity tables can be shown through the following Graph Plots which show the Percentage Drought changes for SPI 6 and SPI 12 cases respectively.

In the above two figures, we can see the percentages of drought severity changes in the historical and predicted periods overall. Moreover, station like Bihar shows a negative percentage change in severe cases as in Fig. 21 and Fatehpur in Fig. 22 shows negative predicted drought in extreme cases.

## 4. Conclusions

This study on meteorological drought was conducted in the southern districts of Bihar. Initially, historical analysis utilized IMD precipitation data, and future climate scenarios were forecasted using outputs from 14 Global Climate Models (GCMs) of CMIP5, which were downscaled and adjusted for the region. In this process, projections for precipitation data were made based on the RCP8.5 greenhouse gas scenarios. To validate the model, a comparison was made between India Meteorological Department (IMD) data and various CMIP5 gridded GCM data for the period 2006-2020. Subsequently, future precipitation data was employed for meteorological drought forecasting using the Standardized Precipitation Index. Our analysis revealed that GCM data demonstrated an accuracy exceeding 72%, indicating reliability. This finding is promising, as it suggests the potential for taking essential measures to address future drought conditions and provide assistance to those in need.

The study can be concluded in the following points:

(i) Examination of historical SPI revealed distinct patterns of severe drought occurrences in various districts of South Bihar. Gaya and Nalanda were affected by three severe drought years each, while Jamui experienced five, Lakhisarai encountered two, and Nawada endured three such extreme events.

(ii) Utilizing MCDM techniques, the performance of Global Climate Models (GCMs) across South Bihar stations was evaluated. Results indicated consistent excellence of the MRI-CGCM3 model, with GISS-E2-H ranking least favourable among the 14 GCMs assessed. Notably, HadGEM2-AO, MRI-CGCM3, MIROC5, CESM1-CAM5, and CCSM4 emerged as the top-performing models.

(iii) Analysis of station-level downscaled precipitation data demonstrated commendable performance, evidenced by $R^2$ values ranging from 0.732 to 0.628 when compared against observed Indian Meteorological Department data.

(iv) Projections for future drought occurrences suggest an escalation in frequency, particularly post-2030. Gaya is anticipated to face four severe drought years, Nalanda two, Lakhisarai one severe to extreme drought, Jamui one severe drought, and Nawada two severe to extreme drought events. These findings underscore the pressing need for proactive measures to mitigate the anticipated impact of these projected droughts on the affected regions.

## 5. Future scope

While the study utilized SPI, future research could explore advanced statistical techniques such as artificial neural networks (ANN) and support vector regression (SVR). These sophisticated methods can potentially enhance the accuracy of drought forecasting, providing more robust insights into future trends. Considering forecasted research, there is a crucial need to develop effective drought mitigation strategies tailored to the specific challenges faced by South Bihar. Future studies should focus on the exploration, assessment, and implementation of feasible and impactful mitigation measures to alleviate the impact of droughts in the region. Acknowledging the uncertainties inherent in GCMs, future investigations should delve into understanding how model uncertainties may influence the accuracy of drought predictions. Ongoing research efforts should focus on the continual refinement and development of more precise GCMs specifically designed for drought forecasting in the South Bihar region. This proactive approach will contribute to the improvement of prediction accuracy and the reliability of future projections.

*Acknowledgement*

The authors would like to thank the Head of Climate Research & Services, India Meteorological Department, Shivajinagar, Pune, and World Climate Research Program's coupled modelling working group and the European Centre for Medium-Range Weather Forecasting for developing and making available their model output.

*Funding*

There is no source of funding from any agencies for this research. There are no financial, personal or professional relationships reported that could have been perceived as influencing the research presented.

*Conflict of Interest*

No conflict of interest was found by the authors which may have influenced the work presented in this manuscript.

*Authors' Contributions*

Hari Prakash: Conceptualization, data collection, data processing, methodology development, statistical analysis, SPI computation, GCM evaluation and ranking, visualization, interpretation of results, and preparation of the original manuscript draft. (*email: hariprakash.rs.civ23@iitbhu.ac.in*).
Dr. Pramod Soni: Supervision, methodology refinement, technical guidance, validation of results, review and editing of the manuscript, and overall research coordination. (*email: Pramod.civ@iitbhu.ac.in*).
Dr. K. K. Pandey: manuscript review and editing, and final approval of the submitted version. (*email: kkp.civ@iitbhu.ac.in*).

*Disclaimer*: The contents and views expressed in this research article are the views of the authors and do not necessarily reflect the views of the organizations they belong to.

**References**


Alamgir, M., Khan, N., Shahid, S. *et al.*, 2020, "Evaluating severity–area–frequency (SAF) of seasonal droughts in Bangladesh under climate change scenarios. *Stoch Environ Res Risk Assess* **34**, 447–464. doi: https://10.1007/s00477-020-01768-2.

Allabakash, S., Lim, S., 2022, "Anthropogenic influence of temperature changes across East Asia using CMIP6 simulations", *Sci Rep*, **12**, 11896. doi: https://10.1038/s41598-022-16110-9.

Anandharuban, P., and L. Elango. 2021. "Spatio-Temporal Analysis of Rainfall, Meteorological Drought and Response from a Water Supply Reservoir in the Megacity of Chennai, India", *Journal of Earth System Science* **130**, 1, 17. doi: https://10.1007/s12040-020-01538-2.

Balaji, V., Taylor, K. E., Juckes, M., Lawrence, B. N., Durack, P. J., Lautenschlager, M., Blanton, C., Cinquini, L., Denvil, S., Elkington, M., Guglielmo, F., Guilyardi, E., Hassell, D., Kharin, S., Kindermann, S., Nikonov, S., Radhakrishnan, A., Stockhause, M., Weigel, T., and Williams, D. 2018, "Requirements for a global data infrastructure in support of CMIP6", *Geosci. Model Dev.*, **11**, 3659–3680, https://doi.org:10.5194/gmd-11-3659-2018.

Chang, Tiao J. 1991, 'Investigation of Precipitation Droughts by Use of Kriging Method'. *Journal of Irrigation and Drainage Engineering* **117**, 6, 935–43. doi.org:10.1061/(ASCE)0733-9437(1991)117:6(935).

Charles, S., R. Silberstein, J. Teng, G. Fu, G. Hodgson, C. Gabrovsek, J. Crute, F. Chiew, I. Smith, and D. Kirono. 2010, 'Climate Analyses for South-West Western Australia'. *A Report to the Australian Government from the CSIRO South-West Western Australia Sustainable Yields Project*. doi: https://10.1002/wcc.577.

Cheval, Sorin, Aristita Busuioc, Alexandru Dumitrescu, and Marius-Victor Birsan. 2014. 'Spatiotemporal Variability of Meteorological Drought in Romania Using the Standardized Precipitation Index (SPI)'. *Climate Research* **60**, 3, 235–48. doi: https://10.3354/cr01245.

Dabanlı, İsmail, Ashok K. Mishra, and Zekai Şen. 2017, 'Long-Term Spatio-Temporal Drought Variability in Turkey'. *Journal of Hydrology*, **552**, 779–92. doi: https://10.1016/j.jhydrol.2017.07.038.

Donegan, H. A., Francis J. Dodd, and T. B. M. McMaster. 1992, 'A New Approach to AHP Decision-Making'. *Journal of the Royal Statistical Society: Series D (The Statistician)* **41**, 3, 295–302. doi: https:///10.2307/2348551.

Edwards, Daniel C. 1997. *Characteristics of 20th Century Drought in the United States at Multiple Time Scales*. Air Force Inst of Tech Wright-Patterson Afb Oh. AFIT-97-051

Fahad, Shah, Muhammad Adnan, Shah Saud, and Lixiao Nie. 2022. *Climate Change and Ecosystems: Challenges to Sustainable Development*. CRC Press. doi: https:// 10.1201/9781003286400

Gidden, Matthew J., Keywan Riahi, Steven J. Smith, Shinichiro Fujimori, Gunnar Luderer, Elmar Kriegler, Detlef P. Van Vuuren, Maarten Van Den Berg, Leyang Feng, and David Klein. 2019. 'Global Emissions Pathways under Different Socioeconomic Scenarios for Use in CMIP6: A Dataset of Harmonized Emissions Trajectories through the End of the Century'. *Geoscientific Model Development* **12**, 4, 1443–75. doi: https://10.5194/gmd-12-1443-2019. , 2019

Gupta, Vivek, and Manoj Kumar Jain. 2018. 'Investigation of Multi-Model Spatiotemporal Mesoscale Drought Projections over India under Climate Change Scenario'. *Journal of Hydrology* **567**, 489–509. doi: https://10.1016/j.jhydrol.2018.10.012.

Guttman, Nathaniel B. 1998. 'Comparing the Palmer Drought Index and the Standardized Precipitation Index 1'. *JAWRA Journal of the American Water Resources Association*, **34**, 1, 113–21. doi: https://10.1016/j.jhydrol.2018.10.012.

Hayes, Michael J., Mark D. Svoboda, Donald A. Wiihite, and Olga V. Vanyarkho. 1999. 'Monitoring the 1996 Drought Using the Standardized Precipitation Index'. *Bulletin of the American Meteorological Society* **80**, 3, 429–38.doi: https://10.1175/1520-0477(1999)080<0429:MTDUTS>2.0.CO;2.

Kalisa, Wilson, Jiahua Zhang, Tertsea Igbawua, Fanan Ujoh, Obas John Ebohon, Jean Nepomuscene Namugize, and Fengmei Yao. 2020. 'Spatio-Temporal Analysis of Drought and Return Periods over the East African Region Using Standardized Precipitation Index from 1920 to 2016'. *Agricultural Water Management* **237**, 106195. doi: https://10.1016/j.agwat.2020.106195.

Kar, Abhipsa, Manas Ranjan Das, and Dipanjali Mohapatra. 2022. 'An Experimental Study on Use of Biopolymer for Sustainable Stabilization of Slopes'. *Materials Today: Proceedings* **62**, 6148–52. doi: https://10.1016/j.matpr.2022.05.027.

Laddimath, Rajashekhar S., and Nagraj S. Patil. 2020. 'Assessment of Future Meteorological Drought in Bhima Basin Based on CMIP5 Multi-Model Projections'. *International Journal of Future Generation Communication and Networking* **13**, 4, 2903–11. ISSN: 2233-7857 IJFGCN

Mahajan, Dattatraya R., and Basavanand M. Dodamani. 2016. 'Spatial and Temporal Drought Analysis in the Krishna River Basin of Maharashtra, India' edited by G. Mannina. *Cogent Engineering* **3**, 1, 1185926. doi: https://10.1080/23311916.2016.1185926.

McKee, T. B., Doesken, N. J., & Kleist, J., 1993, January, "The relationship of drought frequency and duration to time scales. In *Proceedings of the 8th Conference on Applied Climatology*, **17**, 22, 179-183.

Merabti, Abdelaaziz, Diogo S. Martins, Mohamed Meddi, and Luis S. Pereira. 2018. 'Spatial and Time Variability of Drought Based on SPI and RDI with Various Time Scales'. *Water Resources Management* 32(3):1087–1100. doi: https://10.1007/s11269-017-1856-6.

Mishra, A. K., and V. R. Desai. 2005. 'Spatial and Temporal Drought Analysis in the Kansabati River Basin, India'. *International Journal of River Basin Management* 3, 1, 31–41. doi: https://10.1080/15715124.2005.9635243.

Mishra, Ashok K., and Vijay P. Singh. 2010. 'A Review of Drought Concepts'. *Journal of Hydrology* **391**, 1–2, 202–16. doi: https://10.1016/j.jhydrol.2010.07.012.

Mishra, S. Sangita, and R. Nagarajan. 2011. 'Spatio-Temporal Drought Assessment in Tel River Basin Using Standardized Precipitation Index (SPI) and GIS'. *Geomatics, Natural Hazards and Risk* **2**, 1, 79–93. doi: https://10.1080/19475705.2010.533703.

Mujumdar, P.P. and Nagesh Kumar, D., 2012, Floods in a Changing Climate: Hydrologic Modeling,Cambridge University Press, Cambridge, UK,ISBN: 978-1-107-01876-1.

Mundetia, Nitika, and Devesh Sharma. 2015. 'Analysis of Rainfall and Drought in Rajasthan State, India'. *Global Nest J* **17**, 1, 12–21.

Mustafa, Ahmed, and Ghani Rahman. 2018. 'Assessing the Spatio-Temporal Variability of Meteorological Drought in Jordan'. *Earth Systems and Environment* **2**, 2, 247–64. doi: https://10.1007/s41748-018-0071-9.

Newton, Adrian C., Scott N. Johnson, and Peter J. Gregory. 2011. 'Implications of Climate Change for Diseases, Crop Yields and Food Security'. *Euphytica* **179**, 1, 3–18. doi: https://10.1007/s10681-011-0359-4.

Patel, Gaurav, Subhasish Das, and Rajib Das. 2023. 'Identification of Best CMIP5 Global Climate Model for Rainfall by Ensemble Implementation of MCDM Methods and Statistical Inference'. *Water Resources Management* **37**, 13, 5147–70. doi: https://10.1007/s11269-023-03599-6.

Pomerol, J.C. and Barba-Romero, S., 2000,Multicriterion Decision in Management: Principles and Practice,Kluwer Academic Publishers, Dordrecht, The Netherlands,ISBN: 0-7923-7756-7.

Raja, R., A. K. Nayak, B. B. Panda, B. Lal, Rahul Tripathi, Mohammad Shahid, Anjani Kumar, Sangita Mohanty, P. Samal, and Priyanka Gautam. 2014. 'Monitoring of Meteorological Drought and Its Impact on Rice (Oryza Sativa L.) Productivity in Odisha Using Standardized Precipitation Index'. *Archives of Agronomy and Soil Science* **60**, 12, 1701–15. doi: https://10.1080/03650340.2014.912033.

Raju, K. Srinivasa, and D. Nagesh Kumar. 2014. 'Ranking of Global Climate Models for India Using Multicriterion Analysis'. *Climate Research* **60**, 2, 103–17. doi : https://10.3354/cr01222.

Saharwardi, Md Saquib, and Pankaj Kumar. 2022. 'Future Drought Changes and Associated Uncertainty over the Homogenous Regions of India: A Multimodel Approach'. *International Journal of Climatology* 42(1):652–70. doi: https://10.1002/joc.7265.

Salehie, Obaidullah, Mohammed Magdy Hamed, Tarmizi Bin Ismail, Tze Huey Tam, and Shamsuddin Shahid. 2023. 'Selection of CMIP5 GCM with Projection of Climate over the Amu Darya River Basin'. *Theoretical and Applied Climatology* 151, 3–4, 1185–1203. doi: https://10.1007/s00704-022-04332-w.

Santos, Maria Alzira. 1983. 'Regional Droughts: A Stochastic Characterization'. *Journal of Hydrology* **66**, 1, 183–211. https://10.1016/0022-1694(83)90185-3.

Shah, Ravi, Nitin Bharadiya, and Vivek Manekar. 2015. 'Drought Index Computation Using Standardized Precipitation Index (SPI) Method for Surat District, Gujarat'. *Aquatic Procedia* **4**, 1243–49.doi: https://10.1016/j.aqpro.2015.02.162.

Srinivasa Raju, K., and D. Nagesh Kumar. 2015. 'Ranking General Circulation Models for India Using TOPSIS'. *Journal of Water and Climate Change* **6**, 2, 288–99. doi: https://10.2166/wcc.2014.074.

Stagge, James H., Lena M. Tallaksen, Lukas Gudmundsson, Anne F. Van Loon, and Kerstin Stahl. 2015. 'Candidate Distributions for Climatological Drought Indices (SPI and SPEI)'. *International Journal of Climatology* **35**, 13, 4027–40. https://doi.org/10.1002/joc.4267.

St.Clair, Samuel B., and Jonathan P. Lynch. 2010. 'The Opening of Pandora's Box: Climate Change Impacts on Soil Fertility and Crop Nutrition in Developing Countries'. *Plant and Soil* **335**, 1–2, 101–15. doi: https://10.1007/s11104-010-0328-z.

Thom, Herbert CS. 1958. 'A Note on the Gamma Distribution'. *Monthly Weather Review* **86**, 4, 117–22. doi: https://10.1175/1520-0493(1958)086<0117:ANOTGD>2.0.CO;2.

Thomas, T., P. C. Nayak, and Narayan C. Ghosh. 2015. 'Spatiotemporal Analysis of Drought Characteristics in the Bundelkhand Region of Central India Using the Standardized Precipitation Index'. *Journal of Hydrologic Engineering* **20**, 11, 05015004. doi: https://10.1061/(ASCE)HE.1943-5584.0001189.

Van Dijk, Albert IJM, Hylke E. Beck, Russell S. Crosbie, Richard AM De Jeu, Yi Y. Liu, Geoff M. Podger, Bertrand Timbal, and Neil R. Viney. 2013. 'The Millennium Drought in Southeast Australia (2001–2009): Natural and Human Causes and Implications for Water Resources, Ecosystems, Economy, and Society'. *Water Resources Research* **49**, 2, 1040–57. https://doi.org/10.1002/ wrcr.20123.

Vicente-Serrano, Sergio M. 2006. 'Spatial and Temporal Analysis of Droughts in the Iberian Peninsula (1910–2000)'. *Hydrological Sciences Journal* **51**, 1, 83–97. doi: https://10.1623/hysj.51.1.83.

Wilhite, Donald A., and Michael H. Glantz. 1985. 'Understanding: The Drought Phenomenon: The Role of Definitions'. *Water International* **10**, 3, 111–20. doi: https://10.1080/02508068508686328.

Yacoub, Ely, and Gokmen Tayfur. 2017. 'Evaluation and Assessment of Meteorological Drought by Different Methods in Trarza Region, Mauritania'. *Water Resources Management,* **31**, 825–845. doi: https://doi.org/10.1007/s11269-016-1510-8.